University of Mississippi

eGrove

A Modular Data Acquisition Device and Biosignal Amplifier Design

Erin Bratu
University of Mississippi

A Modular Data Acquisition Device & Biosignal Amplifier Design

Erin Bratu

A thesis submitted to the faculty of The University of Mississippi in partial fulfillment of the requirements of the Sally McDonnell Barksdale Honors College.

Oxford
May 2019

Approved By:

_____

Advisor: Dr. Dwight Waddell

_____

Reader: Dr. Glenn Walker

_____

Reader: Dr. Toshikazu Ikuta

DEDICATION

To all my family and all my friends –
I couldn't have done it without you.

ACKNOWLEDGEMENTS

First and foremost, a huge thank you to Dr. Waddell for working with me for the past year, believing in me, and fighting for me so I could focus on my thesis. Additionally, a big thank you to Dr. Ikatu and Dr. Walker for their kind words and advice on finishing up this project. By extension, I am very grateful for all of the electrical engineering faculty and staff for teaching me everything I know and helping me every step of the way.

A wise person once said "Your family is the squad you're born into; your squad is the family you choose." To my family – thank you for everything you have done for me over the past 22 years, especially putting up with me. To my squad – thank you for giving me new life and for always being really rad people. Last but not least, a huge thank you to my cat for her companionship and for (very demandingly) reminding to take a break every now and then to feed both of us.

ABSTRACT

The purpose of this research project is to revise a previous design of a modular data collection device and to develop a biosignal amplifier for use in EEG research. The primary goals of the device redesign were to address the challenges identified at the conclusion of the previous research and to either reaffirm or update various aspects of the implementation – primarily the main components that make up the device. The amplifier circuitry is designed to provide both amplification of the input signals and preliminary filtering of undesirable noise artifacts caused by common environmental sources. Both the collection device and the amplifier circuit were tested individually to verify their viability. These systems are designed to be implemented as part of a larger system, although the specifics of these systems are left up to the requirements of the desired project. This thesis primarily focuses on the design details of these two components.

Contents

List of Figures

LIST OF ABBREVIATIONS

A	Ampere
ABS	Acrylonitrile Butadiene Styrene
AC	Alternating Current
ADC	Analog-to-Digital Converter
API	Application Programming Interface
CLI	Command Line Interface
CMR	Common-Mode Rejection
CMRR	Common-Mode Rejection Ratio
DAQ	Data Acquisition Device
dB	Decibel
DB-25	25-pin D-subminiature
DC	Direct Current
DPST	Double-Pole Single-Throw
ECG	Electrocardiography
EEG	Electroencephalography
EMG	Electromyography
ERP	Event-related Potentials
GUI	Graphical User Interface
h	Hour(s)
Hz	Hertz
IC	Integrated Circuit
IP	Internet Protocol
kS/s	Kilosamples Per Second
mA	Milliampere
mAh	Milliampere Hour
MCC	Measurement Computing Corporation
MΩ	Megaohm
μV	Microvolt
R&D	Research & Development
USB	Universal Serial Bus
V	Volt
Ω	Ohm

Chapter 1

Introduction

Most biosignal data collection currently requires the use of large, expensive devices that are only available in hospital and clinical research settings. Additionally, different measurement tests, such as EEG, ECG, or EMG, typically require unique, specialized systems that cost several thousand dollars each while ultimately performing the same task: data collection. As medical research expands, new applications of these and other tests are being studied, but many of these applications do not call for the same level of precision and expansiveness provided by the medical grade equipment used for diagnoses. Primarily, these applications may generally be accomplished using fewer, more targeted channels. Although simpler data acquisition systems exist, these generally require that the user construct the entire system from scratch, beginning with the data acquisition module and building up according to their needs. Because of this, a modular data acquisition system that provides the baseline operation of the collection functions used in most medical research equipment could be used and adapted to a variety of applications depending upon the user's desire through the supplication of the additional circuitry required by the chosen application.

The aim of this research project is to fulfill this need by improving upon a previous design of a data acquisition system that acts as a single, generalized module of a larger system [3]. This is

accomplished through the generalization of the inputs and outputs of the module to a standardized structure, for which any system may be designed as long as it meets these requirements. This system is designed such that it can be used as an untethered system for applications in which it may be desirable or required for the test subject to be able to move freely. To meet this requirement, a portable power supply and a controller are included in a single enclosure with the data acquisition device. The device is WiFi-enabled and designed to operate headlessly with no built-in GUI, meaning that the controller may only be directly accessed through its CLI from a remote system using the device's established IP address or specified system name. The system is also capable of wirelessly transferring data to a secondary system during ongoing collection, which is advantageous for applications in which real-time monitoring or a form of external feedback is desired. This is also ideal for applications in which resource-intensive data processing may be required during collection, to prevent performance degradation within the acquisition module. Additionally, great focus was placed on using standardized components in order to simplify the design process of future applications.

Because the primary target of this device is for applications involving biomedical measurements, the module provides eight single-ended analog channels. Additionally, the device provides access to the chosen DAQ's +5 V output and several other digital channels which can be used for more complex collection designs. When using all eight channels, the device can achieve a maximum sampling rate of 50 kS/s per channel simultaneously with 16-bit precision across a configurable voltage range, which provides sufficient precision required for many non-diagnostic applications.

To demonstrate a single application of this module within a larger system, a design for signal conditioning circuitry for amplifying and filtering microvolt-scale biosignals, such as EEG data, is also described in this thesis. A general outline of a fully-developed system in which this circuitry would be used is shown in Figure 1.1. This system collects data from electrodes strategically placed to target signals of interest, which are then amplified to both meet the requirements of the data collection module and to take advantage of the significantly larger voltage ranges the DAQ module provides. The data is then transferred to a secondary computer. The majority of the data processing

2
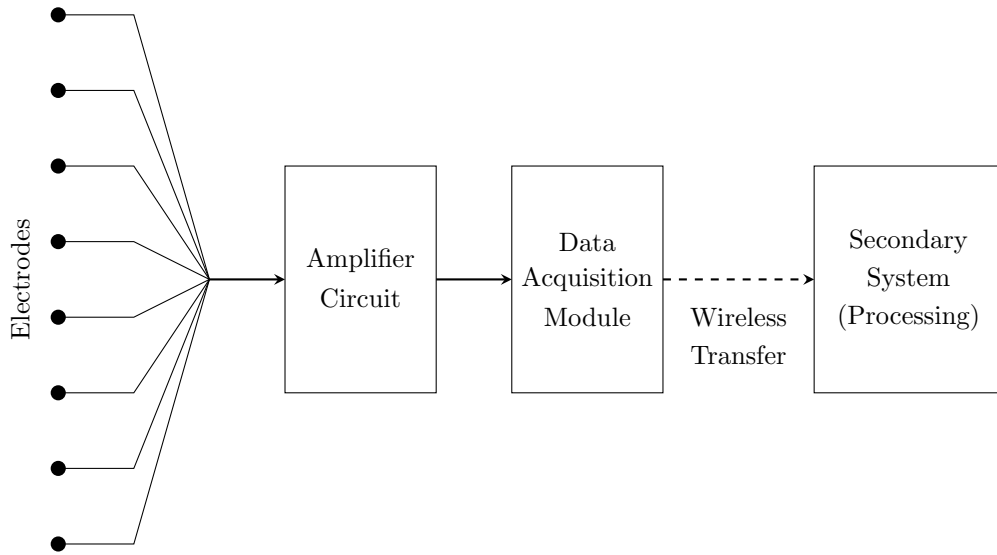
Figure 1.1: Overview of the EEG-based biofeedback system.

occurs at this stage. In EEG applications, this generally includes transforming the signal from the time domain to the frequency domain, allowing users to study specific frequencies. From this point, the data may be applied in a number of applications according to the users' desires, the details of which are beyond the scope of this thesis.

The information in this thesis primarily focuses on the design of both the data collection module and the signal intake and conditioning circuitry, which are described in Chapter 3 and Chapter 4, respectively. Preliminary results for tests of these components are discussed in these chapters as well. A discussion of the outcomes and future work for this project may be found in Chapter 5. Additionally, an overview of the purpose and motivation for this device is provided in the following chapter.

Chapter 2

Background

This thesis continues the work accomplished in a previous thesis that identified several challenges that were unresolved at its culmination. Additionally, it seeks to either reaffirm decisions made for the original design or to improve upon these specifications to create a better device. The design decisions made in constructing the new device are outlined in this chapter. The continued need for such a device is also discussed, highlighting the failure to find a comparable system at a similar price point.

From the previous work done on this topic, the majority of the problems identified involved the enclosure and the design of the device's hardware, although some extended to software as well [3]. The primary issue with the previous device was the internal integrity of the components. When the device was received, several components had become detached from one another through normal movement of the device. Because of this, great emphasis was placed on securing the components in future designs to increase the durability of the device so it can be used reliably in applications that involve the device being used in a non-stationary system, as well as to ensure that the device does not become damaged during normal transport. To resolve these issues, the new enclosure was 3D-printed with an internal structure that was fitted to the individual components, at the cost of

complicating the wiring process and introducing a requirement for precisely measured cable lengths to ensure that there is not any unnecessary tension on the various cables that might degrade the durability of their connections.

In addition to the problems posed by the original enclosure, this project sought to improve upon the original design by expanding the capabilities of the device. The major components of the device were retained in this design as they were deemed comparable to alternative options, but the peripheral connections of the device were overhauled to remove some of the original limitations, such as only being able to connect one probe for data collection. The new design allows for use of all eight analog input channels available on the DAQ, as well as several other channels which will allow for a greater variety of applications. This is discussed in more detail in Section 3.1.4. This project also emphasizes the use of common, standardized connectors to make development of future peripherals simpler.

The software of the device uses an updated version of that which was used in the original, although several changes have been made to the implementation. The new device uses a lighter, minimalist version of the operating system used on the original controller in order to reduce the amount of clutter created by software that will go unused. This decision allows for more refined configuration of the controller, as the user may install only what is needed beyond the base requirements of operation. Additionally, the original device used an ad hoc network to establish Internet connections; this decision has been eliminated in the redesign in favor of establishing static or reserved IP addresses for networks on which the device is used. Although this requires more configuration at the front end, it allows the user to immediately identify whether the device is connected to the network during future use and must only be performed once per network. The scripts used to facilitate data collection have also been streamlined to provide better performance.

One might be wondering what the point of creating such a device is. Currently, there is little to no availability of this type of all-in-one portable data collection module, especially those designed for analog biosignal measurements. Most products in this realm consist only of the data logging device,

such as the one from MCC used in this design, which would have to be put through a design process similar to the one described in this thesis, meaning that off-the-shelf units of this type are largely unavailable in consumer markets. Those that are available and provide similar capabilities as this device are generally cost-prohibitive. Much of the research in this area is being done at the doctoral and professional R&D levels using advanced equipment to create highly customized systems that are intended for use in medical diagnostics. Other research performed at a comparable level to this thesis has produced systems which usually have several deficiencies that are addressed in this design. Primarily, these systems are afflicted by low channel counts, low sampling rates, and limitations on methods of data transmission to a remote system [4–7]. Many of these are also designed with great emphasis on applications for a single measurement type, such as EEG or ECG, rather than on being adaptable to many different applications.

As mentioned previously, the second major focus of this research project is to develop a low-cost EEG hardware system to amplify and filter the collected signals. EEG is a biomedical measurement test designed to measure electrical activity in the brain using electrodes attached to the scalp. Electrodes are typically placed according to locations specified by the International 10-20 system, which spaces electrodes by a distance of either 10% or 20% of the total front-to-back or left-to-right distance of the skull [8]. This layout is shown in Figure 2.1. Activity is measured in the form of neural oscillations, and EEG testing typically focuses on four classes of oscillation activity: delta, theta, alpha, and beta waves. Each wave type is associated with a particular frequency band, spatial location, and activity type, a summary of which is provided in Table 2.1. EEG tests may isolate a certain bandwidth of frequencies and target the activity in this band.

EEG is widely used as a diagnostic tool for patients who are believed to be suffering from epilepsy, a brain tumor, a stroke, or other brain damage or dysfunction [9]. Tests for these conditions are performed in hospitals using large, expensive medical-grade systems. EEG studies mostly focus on ERP, which refers to the brain's response to a certain stimulus or event within a specified timeframe following the event, or an analysis of the neural oscillations described previously.
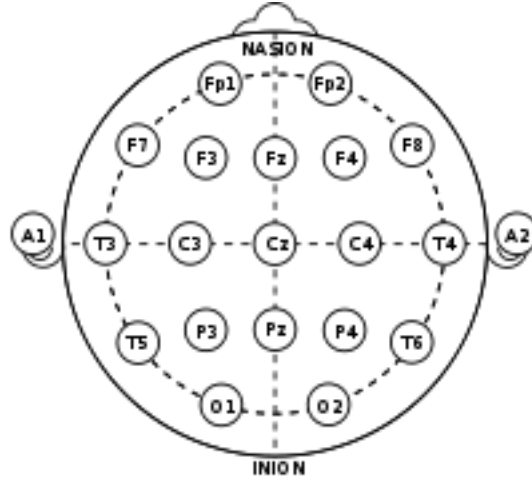
Figure 2.1: The International 10-20 System for EEG Electrode Placement

Wave Type	Frequency Band	Measurement Location	Activity Association
Delta	< 4 Hz	Frontal Regions	Slow-wave sleep
Theta	4-7 Hz	Locations not related to the current task	Drowsiness, idling, suppression of a response or other action
Alpha	8-15 Hz	Posterior Regions	Relaxation, Closing of eyes, inhibition control
Beta	16-31 Hz	Temporal and Frontal Regions	Cognitive processes

Table 2.1: Summary of Common EEG Brainwave Types

The design of signal-conditioning circuitry for EEG signals was selected for this research project due to growing fields of research which use EEG data for non-diagnostic purposes and do not require the same level of precision as medical-grade equipment. It is the group's hope that such a design may be used to provide comparatively low-cost access to an EEG data collection system which is then adapted to the desired application. The group has identified an interest in developing a full system for performing visual biofeedback tests; however, this topic is beyond the scope of this paper, and the design of such a system is left as future work.

As such, this thesis covers only the design and initial isolated tests of the collection device and the conditioning circuitry. A multichannel signal generator is used to simulate the signals which would be provided as inputs to the two components. For the conditioning circuitry, this uses three

signals analogous to those that would be collected by electrodes placed according to the International 10-20 system. One electrode serves as a ground node for the other electrodes and is placed in an electrically-neutral location. The second electrode serves as a reference node that identifies the baseline level of electrical activity in the brain and is usually placed behind the left or right ear, which correspond to locations A1 and A2 in the 10-20 system. The third electrode collects the primary signal of interest and can be placed at different locations on the skull according to the recommendations for targeting certain activities of interest. For the collection device, the signal generator provides a single signal which is representative of the amplified combination of the three inputs to the signal conditioning circuitry, as would be seen at its output. The specifics of these systems are discussed in greater detail in the following chapters.

Chapter 3

Device Design

The primary motivation for designing this device is to create a modular system for analog data acquisition that eliminates the need to have several specialized systems that ultimately perform the same basic tasks. To do this, the redundant components of such systems were isolated from the unique ones to form "modules" of similar tasks which depend on similar inputs and produce similar outputs. The primary module identified was the controller for the data collection, which was developed into a single, enclosed device to which peripheral circuitry or sensors can be attached, depending upon the application. The design described in this chapter builds on the documented work of a previous project, which is found in [3].

3.1 Device Components

The following sections will discuss the features and functions of each of the major components chosen for the device, as well as the reasons for which they were chosen. An overview of this design is shown in Figure 3.1.
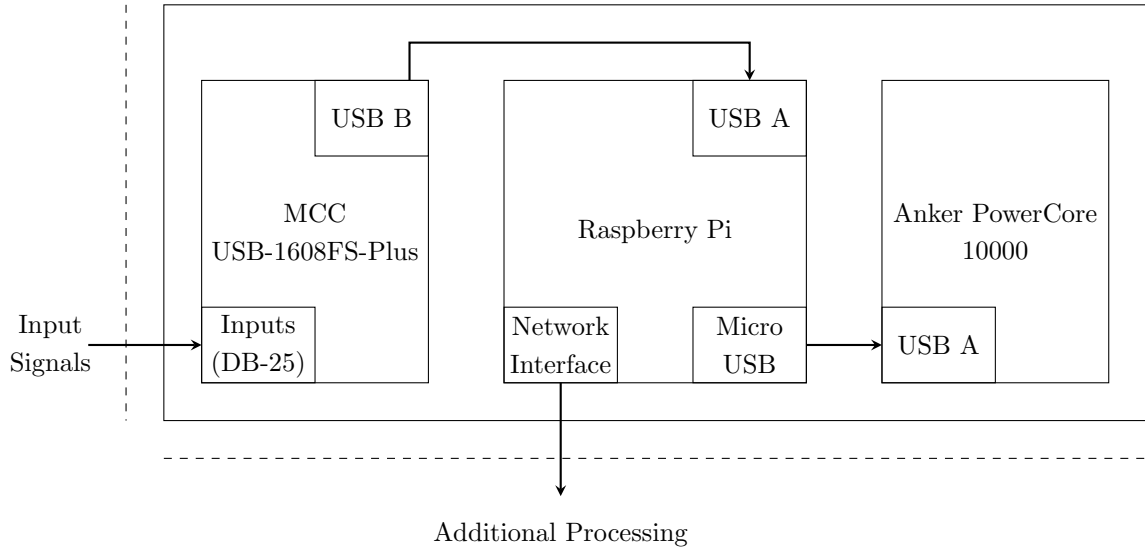
Figure 3.1: Overview of the device design, showing connections between components.

3.1.1   Raspberry Pi 3.0 Model B

An important factor in designing this device was to sacrifice as little as possible in the quality of data collection and processing for the sake of modularity. Because the functions of the device are few and relatively simple, a simple computer without many extraneous functions was desirable, as it would reduce processing delays which may occur in more complex systems. The Raspberry Pi (shown in Figure 3.2) was selected as the main controller of the device for its low cost, simplicity, and customizability. Although the Pi can be used as a stand-alone desktop computer, the undesired functions can also be removed or disabled to provide focus on those which are most important. The Pi also has WiFi capabilities which make interfacing with a secondary computer simple. With these features, the Raspberry Pi can control the configuration of the DAQ, start and stop data collection, perform data processing, and transfer data to a secondary computer for more intensive processing or other purposes.
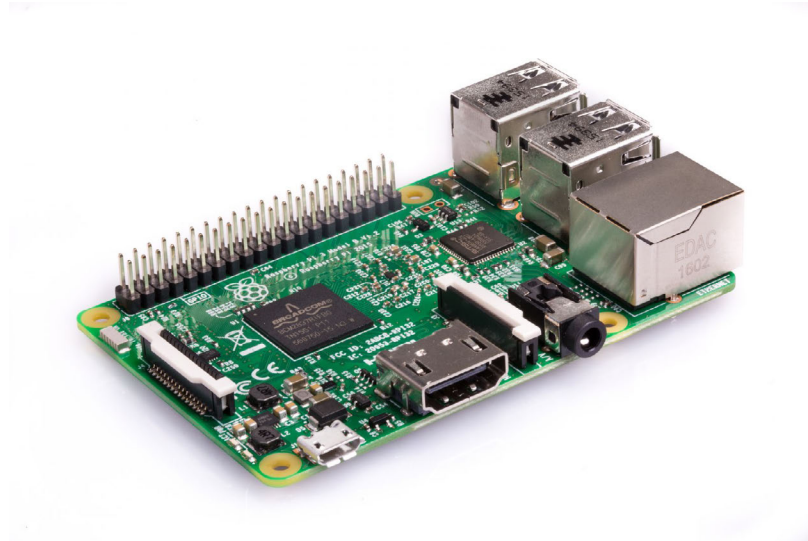
Figure 3.2: Raspberry Pi Model 3 B

3.1.2   MCC USB-1608FS-Plus

For the device, a DAQ primarily functions as the data collector and as an ADC. The MCC USB-1608FS-Plus, which can be seen in Figure 3.3, was selected because it is a low-cost data acquisition system which provides the necessary precision required for many applications. It has 8 digital input channels and 8 single-ended analog input channels, as well as 16-bit resolution over the selectable voltage ranges of ± 1, ± 2, ± 5, or ± 10 V. The maximum sampling rate of this model is 400 kS/s across all 8 analog input channels, with a maximum of 100 kS/s for a single channel. The pinout of this device is shown in Figure 3.4. The DAQ is compatible with Linux, Android, and Windows systems and has software libraries in both C and Python, which will be discussed further in Section 3.2. [1]

Figure 3.3: MCC USB-1608FS-Plus, non-OEM model
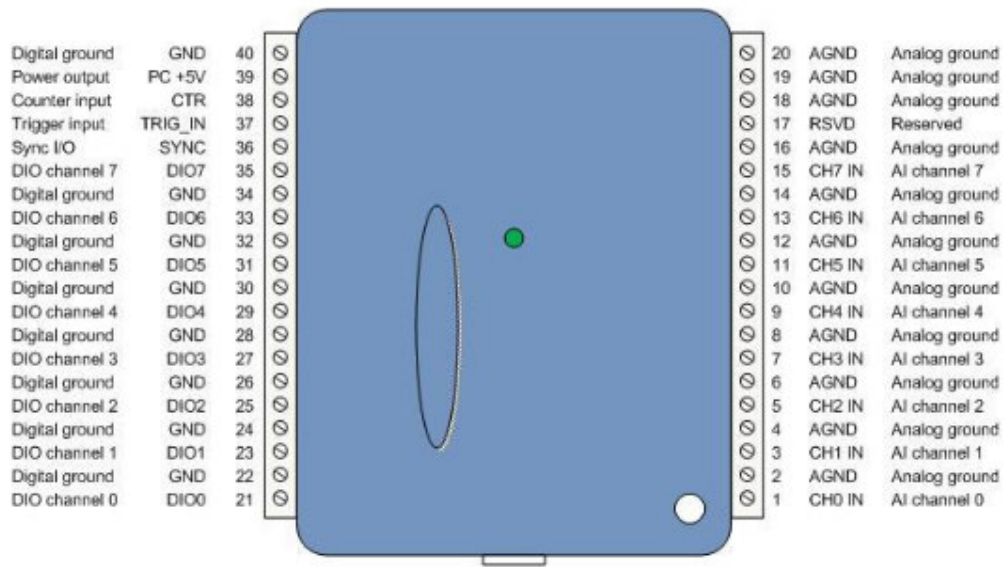
Figure 3.4: Pinout of the MCC USB-1608FS-Plus [1]

3.1.3 Anker PowerCore 10000

Because some applications of this device may require it to be untethered, it requires a portable power supply which is small, lightweight, and rechargeable. Figure 3.5 shows the Anker PowerCore 10000 rechargeable battery, which was selected because it fulfilled all of the stated requirements

while staying within the confines of cost considerations. This battery provides 10000 mAh of charge with a maximum output voltage of 5 V and maximum output current of 2.4 A [10]. Ideally, the device should be able to collect data for several hours on a single charge of the battery, which can be determined from the power requirements of the Raspberry Pi and the DAQ. Documentation for the chosen model of the Raspberry Pi lists the typical bare-board active current consumption at 400 mA and the maximum total USB peripheral current draw as 1.2A, with a recommended current supply of 2.5 A [11]. The selected MCC DAQ requires a supply current between 100 mA and 500 mA [1]. From these values, a range of projected battery life may be calculated using the following equation:

$$Battery\ Life\ (h) = \frac{Battery\ Capacity\ (mAh)}{Current\ Drawn\ (mA)} \qquad (3.1)$$

Using the extreme ranges of these values, the selected battery would be capable of powering the Raspberry Pi for 25 h with no USB peripherals and 6.25 h at the maximum USB peripheral current draw. However, operation at either end of this spectrum is unlikely. From the supply current specifications of the MCC DAQ above, a better estimation of the range of current draw is 600 mA to 1000 mA, for which the Anker battery could ideally supply between 10 and 16.67 h of power. Finally, because the battery is designed to be always-on when connected to a current-drawing output and no data transfer is required between it and the Pi, the connection between the battery and the Raspberry Pi is formed using charge-only USB cables and a single 4-pin DPST switch to control current flow.

Figure 3.5: Anker PowerCore 10000

3.1.4 Peripherals & Interfacing

A device is only as useful as its inputs and outputs, so the methods of interfacing this device with its inputs and outputs were thoughtfully selected to minimize difficulties across these thresholds. This includes the use of common, widely-available resources to create these interfaces. The simplest interface of the entire device is that used to recharge the power supply, which is created using a male-to-female Micro-B USB adapter to extend the original charging port of the power supply to a more convenient external location on the device's enclosure. However, the remaining interfaces are much more complex and will be discussed in detail below.

Input Interfaces

The primary input interface connects the DAQ to the external input signals for which data are being collected. The main goals in designing this interface were to utilize as many of the available I/O terminals on the DAQ as possible while minimizing the size of the physical interface and still using standardized components, all of which were shortcomings of the original design. A 25-pin micro-D connector was chosen to satisfy these requirements. The micro-D connector is a smaller

version of the more common D-Subminiature connector, which is commonly used in applications involving analog signals. Because of their small size, connectors that were pre-wired with 26 AWG stranded wire were selected to reduce problems that may be introduced by hand-constructing them. Although these are standardized connectors, the applications for which they are used does not have a standard pin configuration. The chosen pin layout is illustrated in Figure 3.6, which shows the numbering of the pins,and Table 3.1 lists the corresponding DAQ terminal names for each connector pin, according to those given in Figure 3.4.
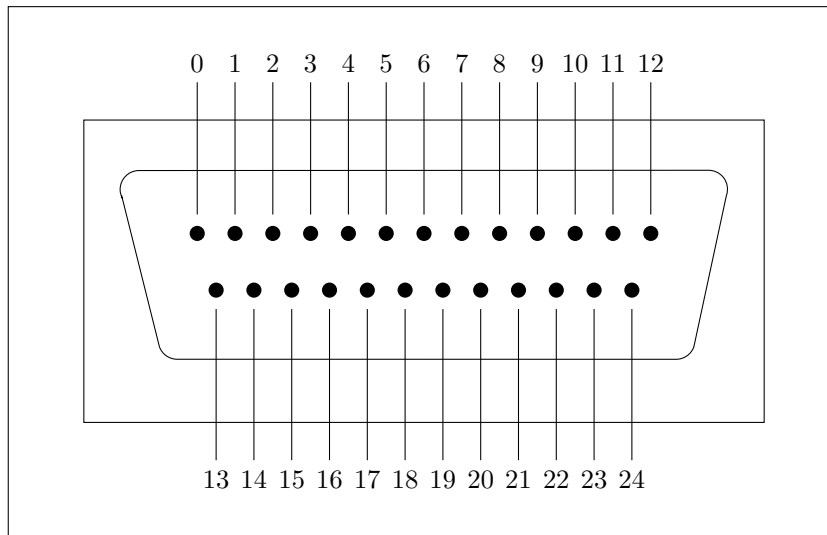
Figure 3.6: Numbering of pins on the 25-pin micro-D socket

Output Interfaces

To limit the amount of data processing performed directly on the Raspberry Pi, the device is designed such that data can be transferred continuously during collection over a wireless network to a secondary system using the IEEE 802.11 WiFi standard. This allows use of the device in applications which require high sampling rates and large volumes of data that need intensive post-processing, in order to reduce the likelihood of introducing a processing delay during the data collection. This also allows it to be used for applications which are intended to provide an immediate output that cannot be supplied by the Raspberry Pi. It is recommended that, when possible, a static IP address

Pin Number	Value	Pin Number	Value
0	AI channel 0	13	Analog Ground
1	AI channel 1	14	Analog Ground
2	AI channel 2	15	Analog Ground
3	AI channel 3	16	Analog Ground
4	AI channel 4	17	Analog Ground
5	AI channel 5	18	Analog Ground
6	AI channel 6	19	Analog Ground
7	AI channel 7	20	Analog Ground
8	Analog Ground	21	Analog Ground
9	Analog Ground	22	Counter Input
10	Sync I/O	23	Trigger Input
11	+5V Power Output	24	Digital Ground
12	No Connection		

Table 3.1: Table of pin numberings (as given in Figure 3.6) and corresponding DAQ terminal values

be obtained for each wireless network to which the device is connected to simplify the networking setup. In addition to the ability to transmit data over a network connection, a secondary method for transferring data over one of the Raspberry Pi's USB Type-A ports is included for situations in which a network connection is unavailable, and the device does not necessarily require being untethered.

3.2 Software

3.2.1 Operating System

The Raspberry Pi runs the Raspbian Stretch Lite operating system, which is specifically designed for the Raspberry Pi and is based on the Debian distribution of Linux. The lite version of the Raspbian Stretch operating system omits several aspects of the full desktop version, including several pre-installed software and the desktop GUI. Because interaction with the device is primarily

intended to be done over a wireless network, the desktop GUI is largely unnecessary as most tasks can be accomplished using the available CLI. This eliminates many unneeded processes running on the Pi's processor, which frees space to be used during data collection.

3.2.2   Networking

The original device design used an ad hoc networking system to provide an Internet connection to the device [3]. The redesign chose to eliminate this system in favor of using statically defined IP addresses for the networks on which the device is used through the reservation of an IP address on the network router at the time of setup. Although this is more work on the front end, it ensures a consistent IP address and eliminates the need to discern the IP address of the device each time it is powered on.

3.2.3   MCC Universal Library for Linux

MCC provides an open-source C/C++ library for controlling and interacting with the company's DAQ products, which can be acquired by installing the uldaq package. In addition to this library, an API providing Python support is also available. Original programs may be written on the Pi for specific applications, or users may opt to use one of the available examples which provide the basic functions of controlling the DAQ. Because of the API and the ease of networking in Python, the majority of programming for the device is done in Python. The code used to control the DAQ in this system may be seen in Appendix A.

The code begins by identifying all available DAQ devices connected to the Raspberry Pi. The program on the remote computer is started first, which then starts the associated program on the Raspberry Pi. Using the information provided by the MCC DAQ library about the device in combination with user-supplied parameters, the collection process is established. The program scans the desired range of channels and packages this data into a single string for transmission. Once the

program is ready to transmit data, it uses an established TCP connection to send the information to the remote computer. This transmission process uses two-way communication to provide control functions for the starting and stopping of the collection process, including verification messages to indicate that the remote computer is still collecting data. The programs are designed such that the program on the Raspberry Pi ends gracefully once the transmission connection ends to prevent unexpected problems caused by unfinished processes.

3.3   Case Design

One of the primary goals of this project was to improve the enclosure of the device in terms of size, organization, and durability. Many of the issues with the original enclosure fall into these categories. Specifically, the enclosure was not optimized for the components, creating an ill fit that necessitated a larger enclosure than necessary and negatively impacted the durability of the device, as several wires were under extra tension which caused them to loosen from their terminals. To address these problems most effectively, additive manufacturing in the form of 3D printing was used to design the new enclosure such that the internal structure was designed according to the shapes of the individual components to provide more stability for the wiring. The AutoCAD design and drafting software from Autodesk were used to generate the design, the final version of which is shown in Figure 3.7. The enclosure was printed on a Fusion3 F400 3D printer using 1.75mm diameter ABS plastic filament from 3DXTech.

From the second iteration of the new enclosure, few major changes have occurred. Successive iterations were focused on the addition of various features and refining the measurements to ensure components have a secure but comfortable fit. The final result of this design process is shown in Figure 3.8. The enclosure is fastened using two #6 standard screws and cap nuts of the corresponding size. To the right of the fastener is the micro-D connector. The front panel of the box contains the power switch for the device as well as an opening for an extension of a USB Type A port on the
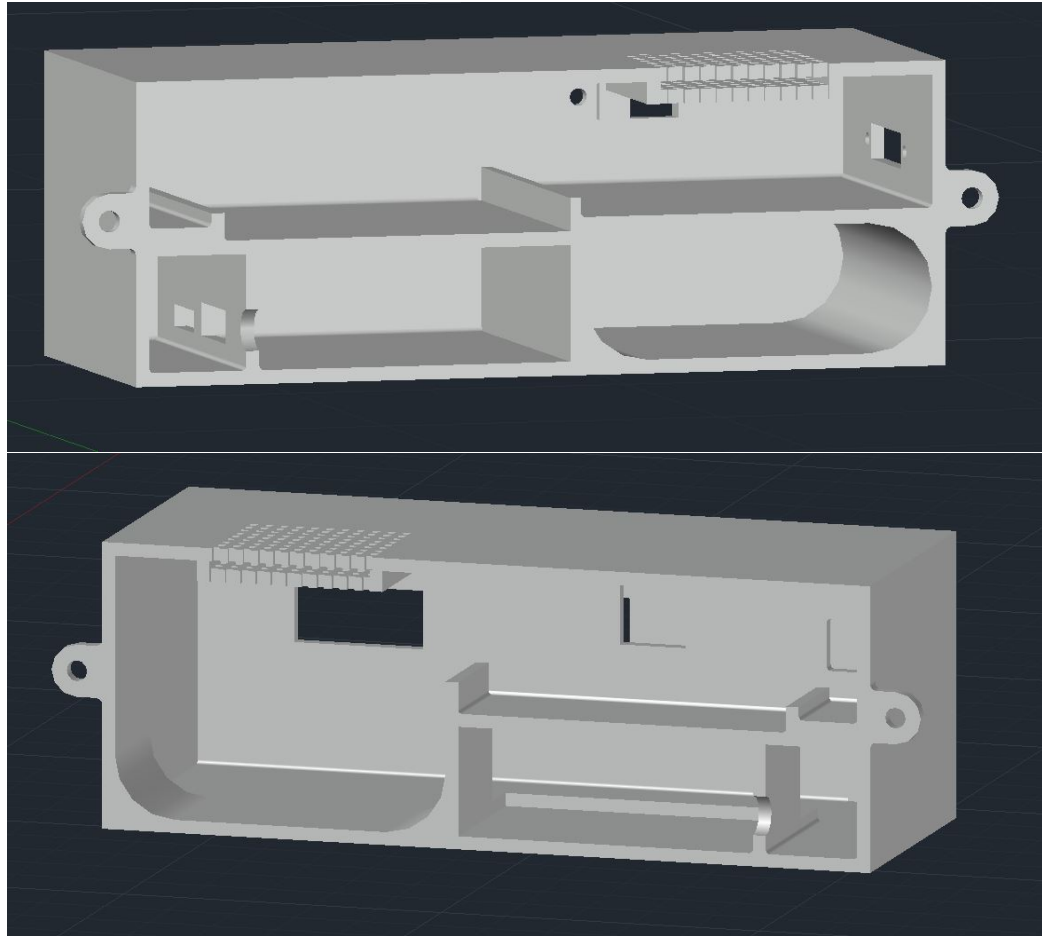
Figure 3.7: A CAD model of the final version of the new enclosure

Raspberry Pi. Although not pictured, the back panel of the device contains the charging extension for the power supply. The main body of the enclosure measures 150mm x 117 mm x 55 mm. This satisfies the objective of reducing the size of the original enclosure, while also increasing the number of available ports on the device.

Figure 3.8: Depiction of the final constructed device.

Chapter 4

Amplifier Design

When operating in the ± 1 V range, the minimum voltage step of the MCC DAQ is 30.5 μV with a total of 65,536 steps. However, because EEG measurements can range from 10 μV to 100 μV, the signal must be amplified to make better use of the precision provided by the DAQ. This can be accomplished using a multistage amplifier. For this particular design, the amplifier was separated into two stages. The first stage is an instrumentation amplifier based on the 3-operational-amplifier design, which will provide the difference between the desired signal and a reference node in order to eliminate the common voltage between them. The second stage uses a non-inverting operational amplifier to amplify the signal to fill most of the ± 1 V range. Additional circuitry was added to provide some preliminary filtering of noise below 0.16 Hz and above 50 Hz. Finally, a notch filter was added to reduce the presence of noisy signals near 60 Hz, which generally stem from environmental sources, such as mains power lines. Figure 4.1 provides an overview of the stages of this amplifier design.
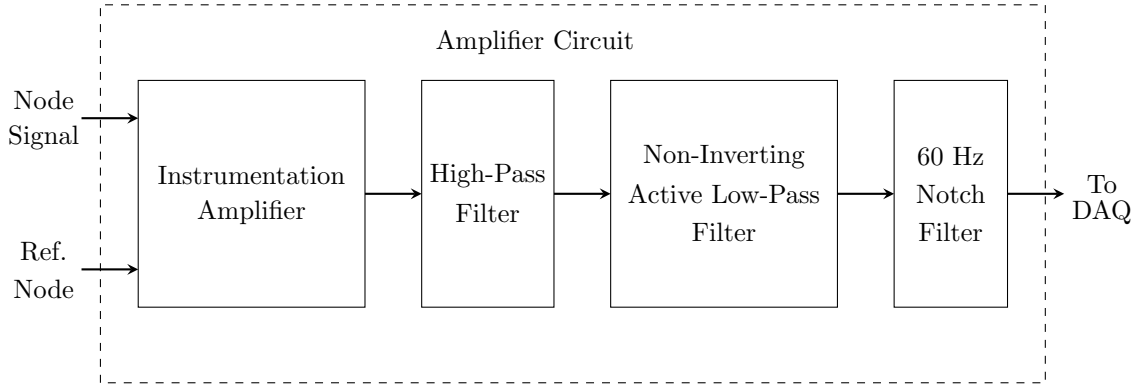
Figure 4.1: Overview of the amplifier circuity.

4.1 Theory

4.1.1 Instrumentation Amplifier

Although it is not required to use an instrumentation amplifier for EEG applications, it provides many advantages over operational and differential amplifiers while also allowing a simpler, less-restricted design process. Primarily, instrumentation amplifiers provide several very desirable characteristics, such as high gain, high input impedance, high CMRR, low noise, low DC offset, and low drift. Additionally, instrumentation amplifier ICs provide more precise gain because most of the resistors are internal to the IC and are very closely matched. Other types of amplifiers are generally not designed with these factors as a priority, so although the base amplifier may initially be more simple, circuits using these amplifiers generally require more design considerations and are overall less accurate than an analogous instrumentation amplifier circuit. As an example, creating a similar circuit with a regular differential amplifier would require the use of very large resistors – on the order of 1 MΩ – which are, by their very nature, far more noisy and more difficult to match than the internal resistors of an instrumentation amplifier IC.

The above characteristics are specifically desirable for biosignal applications for several reasons. For one, high input impedance compared to the source impedance helps mitigate signal distortion

caused by loading effects by ensuring that as much of the incoming voltage signal as possible is conveyed to the amplifier circuit. The CMRR refers to the ability of an amplifier to amplify the difference between two incoming signals while ignoring what is "common" between them, i.e. simultaneous, in-phase signals. For a single pair of electrodes in an EEG application where one electrode represents the primary signal of interest while the other is placed in a relatively electrically-neutral location to be used as a reference node, a high CMRR ensures the removal of most of the baseline electrical signal produced by the body so that the signal coming from the non-reference electrode can be studied more accurately. Additionally, as mentioned previously, high, precise gains and low noise are also extremely important for EEG applications due to the small amplitudes of the initial signals. Finally, almost all EEG activity of interest falls in the 0.16 Hz to 100 Hz frequency band. At the lowest end of this range, where signals begin to look very similar to DC signals at small amplitudes, having a low DC offset is important so that the amplitude range is centered reasonably close to zero to provide the maximum dynamic range in both the positive and negative directions.

Now that the advantages of the instrumentation amplifier have been established, the structure of the amplifier can be discussed. The circuit used in this design uses an instrumentation amplifier which is based on 3 operational amplifiers (op-amps), although the final circuit uses an IC amplifier; however, it is still important to understand the theory behind this design, the basic structure of which is shown in Figure 4.2. The 3 op-amp design uses two non-inverting buffer amplifiers at the inputs, the outputs of which feed into a third op-amp, which acts as a differential amplifier to produce the desired output signal. The circuit also typically consists of three sets of matched resistors and one additional resistor to control the gain, although one could choose to use seven unique resistor values.

The total theoretical gain of the instrumentation amplifier can be calculated by combining the gains found from isolating each of the three op-amps and solving each under the assumption that it is an ideal op-amp. Using the naming system established in Figure 4.2, the gain from v_1 to v_{o1} when $v_2 = 0$ can be found from the following equation:
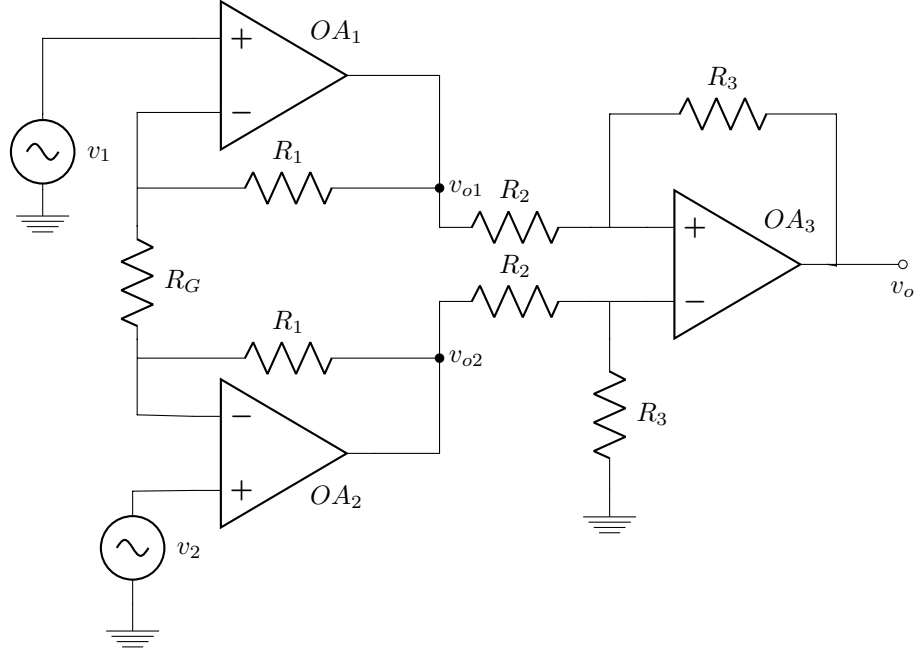
Figure 4.2: Basic structure of the 3 op-amp instrumentation amplifier circuit

$$\frac{v_{o1}}{v_1} = \frac{R_G + R_1}{R_G} \tag{4.1}$$

Similarly, the gain found from v_2 to v_{o2} when $v_1 = 0$ can be found using:

$$\frac{v_{o2}}{v_2} = \frac{R_G + R_1}{R_G} \tag{4.2}$$

The third op-amp acts as a differential amplifier, so the gain of this amplifier is found from the difference of v_{o2} and v_{o1} to v_o, from:

$$\frac{v_0}{v_{o2} - v_{o1}} = \frac{R_3}{R_2} \tag{4.3}$$

After finding each of these individual gains, the overall gain of the instrumentation amplifier may be found by substituting Equations 4.1 and 4.2 into Equation 4.3. This equation, which represents

the gain from the difference of the input signals v_1 and v_2 to v_o, is shown in Equation 4.4.

$$\frac{v_o}{v_2 - v_1} = \frac{R_3}{R_2}\left(1 + \frac{R_1}{R_G}\right) \tag{4.4}$$

4.1.2 High-Pass Filter

Between the instrumentation amplifier and non-inverting active low-pass filter stages, a passive high-pass filter is included to attenuate signals below 0.16 Hz. This is a very simple circuit, but it is helpful in reducing the amount of noise from DC sources that continues into the rest of the amplifier circuit. This circuit is shown in Figure 4.3.
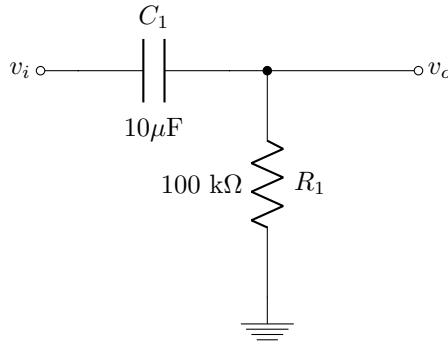
Figure 4.3: High-pass filter circuit designed to attenuate signals below 0.16 Hz.

For this design, the cutoff frequency may calculated using the relation:

$$\omega = \frac{1}{R_1 C_1} \tag{4.5}$$

where ω is the angular frequency, which is equivalent to $2\pi f$, where f is the frequency in Hz. Solving Equation 4.5 for f produces the following result:

$$f = \frac{1}{2\pi R_1 C_1} = \frac{1}{2\pi(100k\Omega)(10\mu F)} = 0.159 Hz \tag{4.6}$$

4.1.3 Non-Inverting Active Low-Pass Filter

The final stage of the amplifier circuit is a non-inverting active low-pass filter, the schematic of which is shown in Figure 4.4. The low-pass filter is designed to attenuate signals above the cutoff frequency, which can also be calculated using Equation 4.6. The filter is said to be active because it is connected to an op-amp circuit which amplifies the incoming signal in addition to the filter, and it is non-inverting because the incoming signal enters the op-amp at the positive terminal.

The gain for this stage may be calculated using the assumption of an ideal op-amp by calculating the total impedance of R_1 and C_1 in parallel and solving the circuit for v_o/v_i. First, the total impedance across C_1 and R_1 is calculated using

$$Z_1 = \frac{R_1 X_C}{\sqrt{R_1{}^2 + X_C{}^2}} \tag{4.7}$$

where X_C is the capacitive reactance of C_1, which can be calculated from

$$X_C = \frac{1}{2\pi f C_1} \tag{4.8}$$

The total impedance can then be used in place of the parallel components to solve for the gain of the circuit, which is given by

$$\frac{v_o}{v_i} = \frac{R_2 + Z_1}{R_2} \tag{4.9}$$

Together, these equations in combination with Equation 4.6 can be used to find the values of R_1, R_2 and C_1 that produce the desired gain and cutoff frequency.
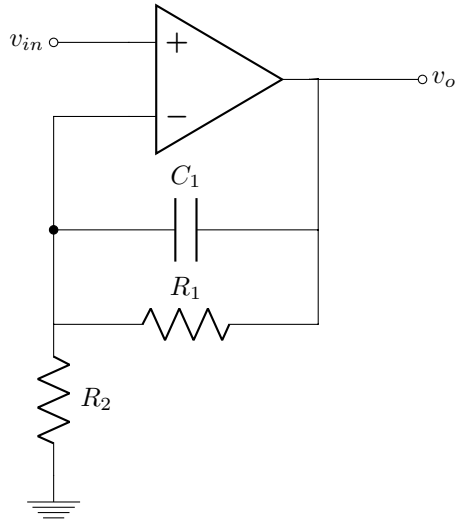
Figure 4.4: Theoretical schematic for the non-inverting active low-pass filter

4.1.4   60 Hz Notch Filter

At the output of the active low-pass filter circuitry is a 60 Hz notch filter. The notch filter creates a dramatic drop-off in the magnitude of signals near to the specified notch frequency, which is 60 Hz in this application. This circuitry was added to reduce undesirable noise from the environment which might complicate the process of isolating the desired signals. Figure 4.5 shows the generalized schematic for a notch-filter. The notch frequency can be used to calculate resistor and capacitor values using the equation

$$f_N = \frac{1}{4\pi RC} \tag{4.10}$$
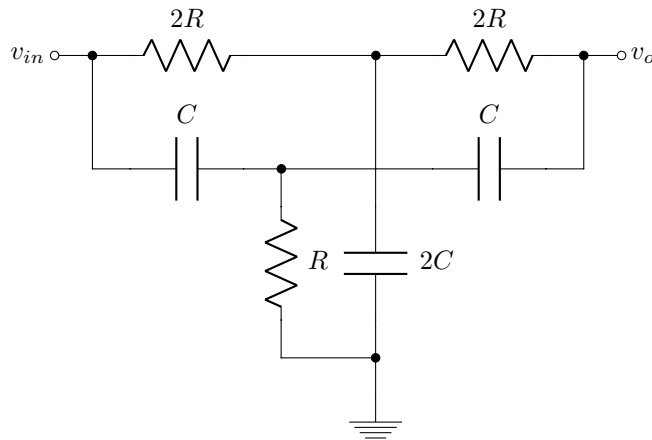
Figure 4.5: Theoretical schematic for a notch filter

4.2 Multisim Simulations

After determining the desired values from the equations outlined in Section 4.1, components were selected and schematics were created in Multisim to test these values. Prior to constructing the full circuit, each stage of the amplifier was constructed and tested separately. The results of these tests, as well as those for the full circuit, are documented in the following subsections.

4.2.1 Instrumentation Amplifier

The primary component of the instrumentation amplifier is the Analog Devices AD623BN instrumentation amplifier IC, the pin layout of which is shown in Figure 4.6. Figure 4.7 shows the Multisim schematic for the isolated instrumentation amplifier circuit. The

Figure 4.6: Pin layout of the AD623BN

AD623BN is a low power, low noise three op-amp instrumentation amplifier that may be used with either single or dual power supplies. The gain is set via a single resistor, the desired value for which can be determined using the equation $R_G = 100 \ k\Omega/G - 1$. From this, it was found that a 499 Ω resistor should be used to achieve a gain of approximately 200. Additionally, the documentation for the AD623BN recommends connecting both $+V_S$ and $-V_S$ to grounded 0.1 μF and 10 μF bypass capacitors. The high-pass filter circuitry can also be seen at the output of the amplifier. [12]

The inputs of the amplifier simulate the signals coming from the electrodes, which have a separate ground from the rest of the circuit. The first signal, with node name V_{in}, represents the signal of interest, and the signal entering the negative terminal of the amplifier represents the reference electrode. For simplicity in simulating the circuit, the reference electrode was connected directly to ground, and the signal electrode was set to 100 μV_{pp} at a frequency of 10 Hz.
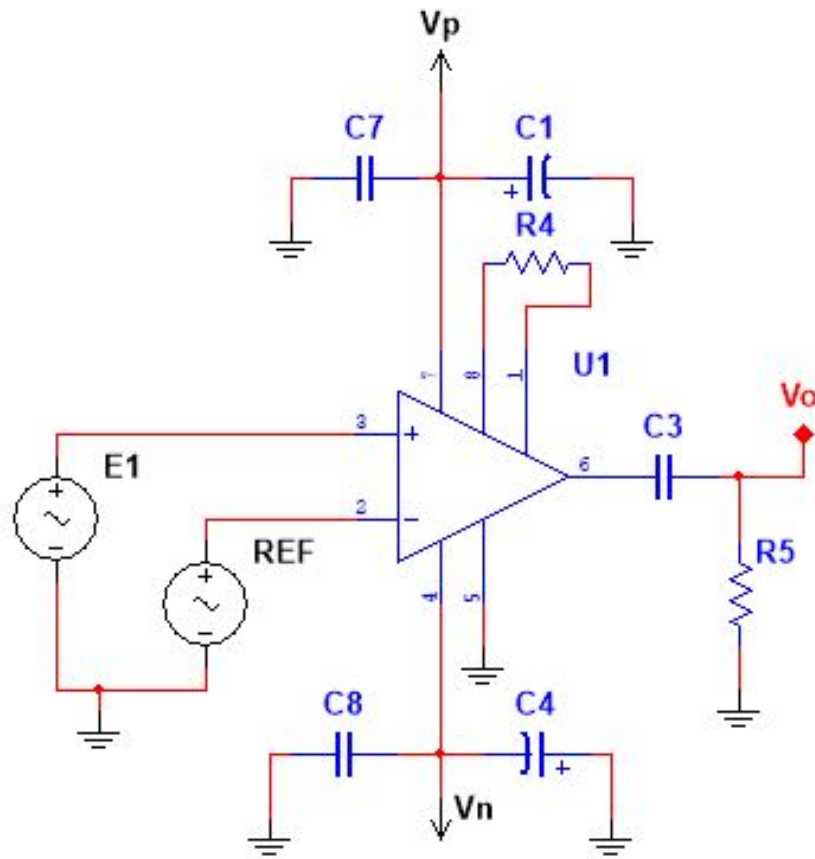
Figure 4.7: Multisim schematic of the instrumentation amplifier.

Figure 4.8 shows the transient response of this circuit. V_o shows a peak output of approximately 20 mV, which is 200 times the maximum of the input signal V_{in}, verifying that the gain resistor selection is accurate. Figure 4.9 shows the magnitude in dB and Figure 4.10 shows the phase in degrees of the input and output signals for frequencies between 1 mHz and 250 Hz. Because the high-pass filter is located after the first stage of amplification, one would expect the signals below the cutoff frequency to be only slightly diminished and shifted out of phase rather than removed entirely, which is confirmed by the graphs.
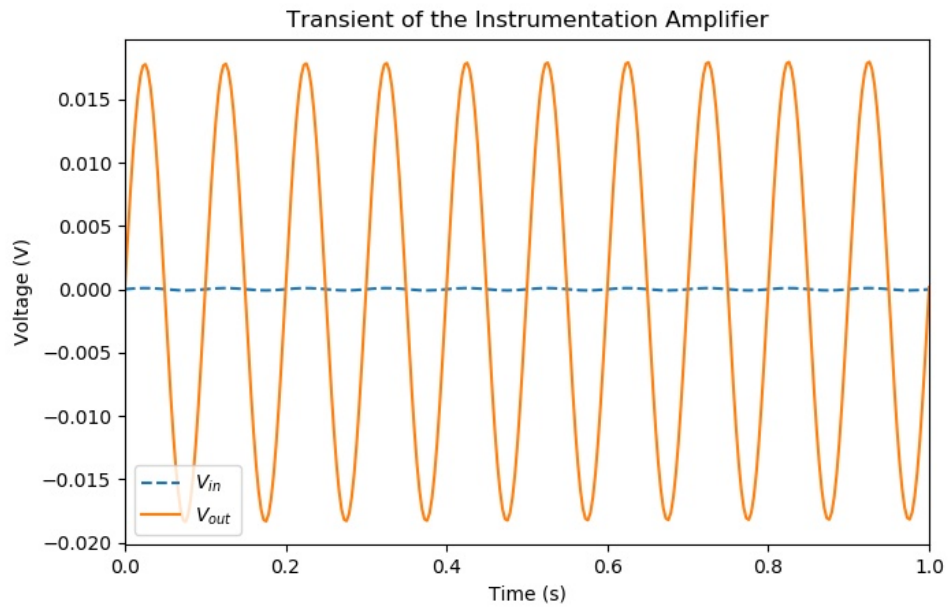
Figure 4.8: Transient response of the circuit shown in Figure 4.7
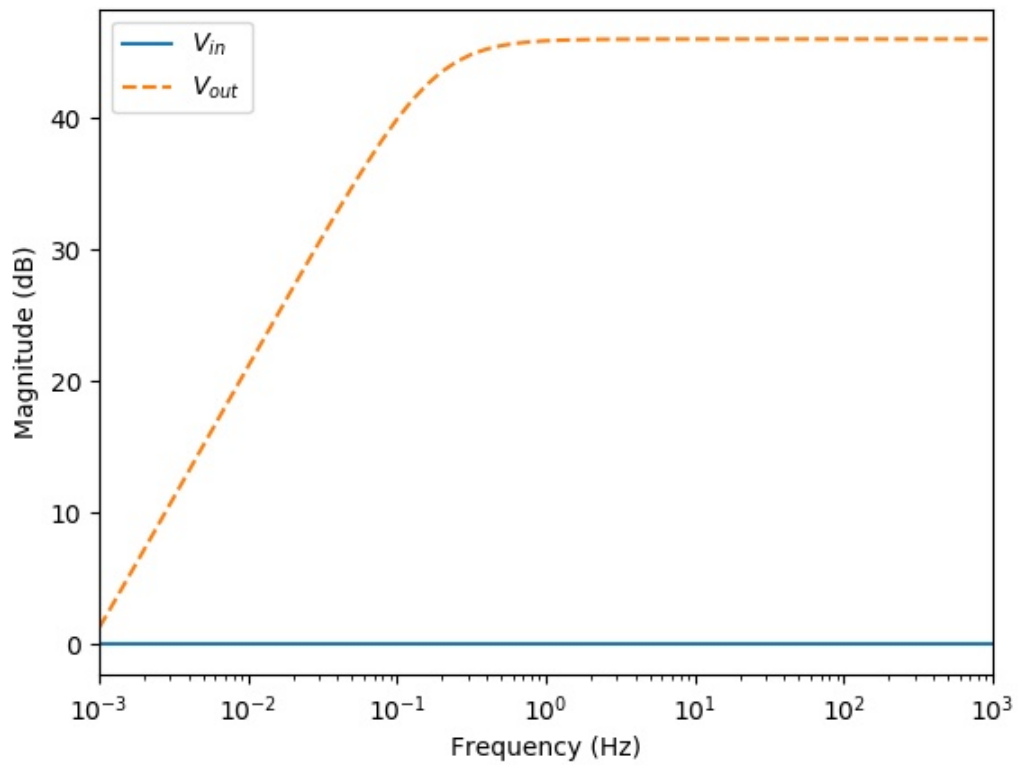
Figure 4.9: Magnitude plot (in dB) from 1 mHz to 1 kHz for the circuit shown in Figure 4.7
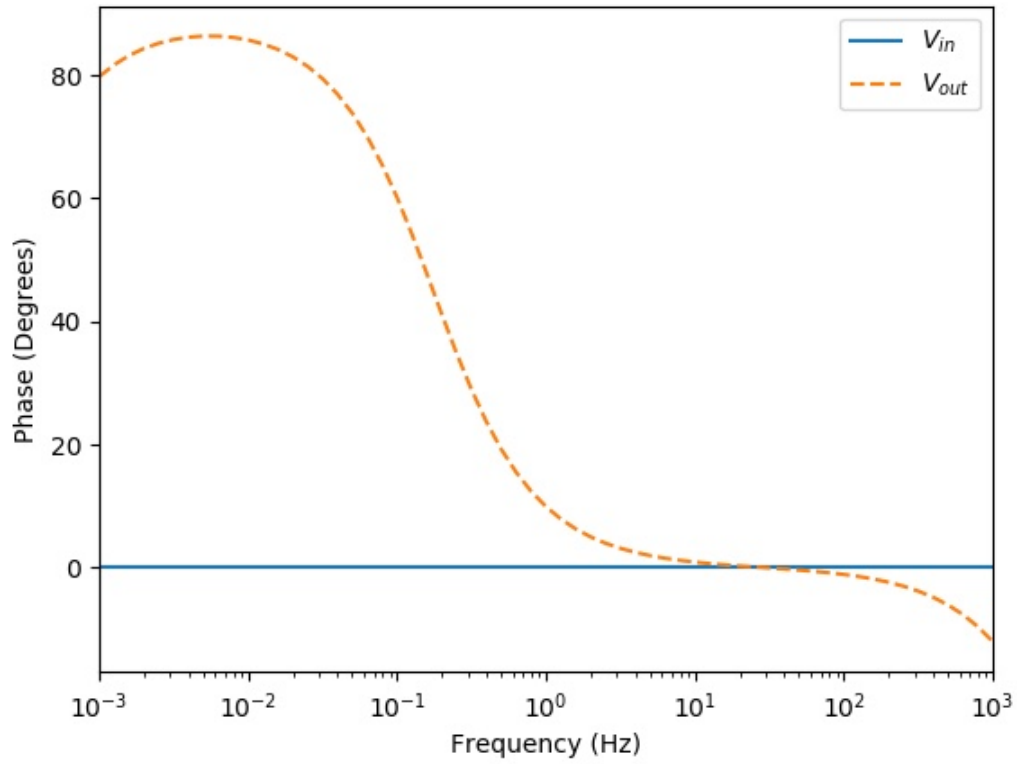
Figure 4.10: Phase plot (in degrees) from 1 mHz to 1 kHz for the circuit shown in Figure 4.7

4.2.2 Non-Inverting Active Low-Pass Filter

Figure 4.12 shows the Multisim schematic for the second stage of the amplifier circuit. The primary component of this stage of the circuit is the TLC277CP IC from Texas Instruments, the pin layout of which is shown in Figure 4.11.
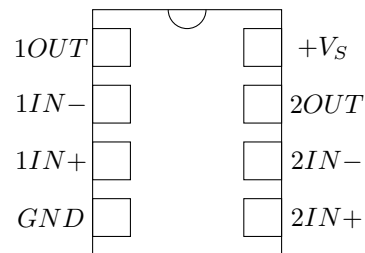
Figure 4.11: Pin layout of the TLC277CP

The positive input signal reflects the output of the instrumentation amplifier, the maximum of which is approximately 20 mV with the selected input and gain values. From the equations in

Section 4.1, it was determined that a 1 μF capacitor and a 3.16 kΩ resistor connected between the negative and output terminals of the op-amp would provide the desired cutoff frequency. From these values, a resistor value of 62 Ω was chosen to provide the desired gain of 50.
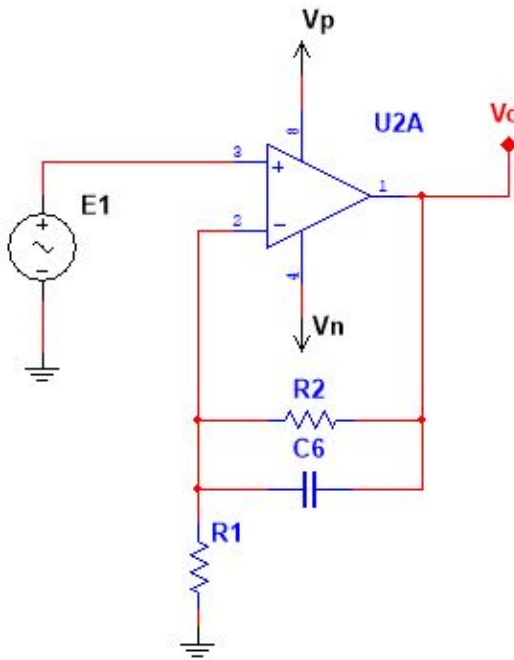
Figure 4.12: Multisim schematic of the non-inverting low-pass filter.

Figure 4.13 depicts the transient response of the low-pass filter, which shows the output signal amplified to ±1 V, corresponding to the theoretical gain of 50. Additionally, Figures 4.14 and 4.15 show the magnitude and phase, respectively, of the input and output signals over the range of 1 mHz to 250 Hz, which shows attenuation of signals above 50 Hz at a rate of approximately -20 dB/decade.
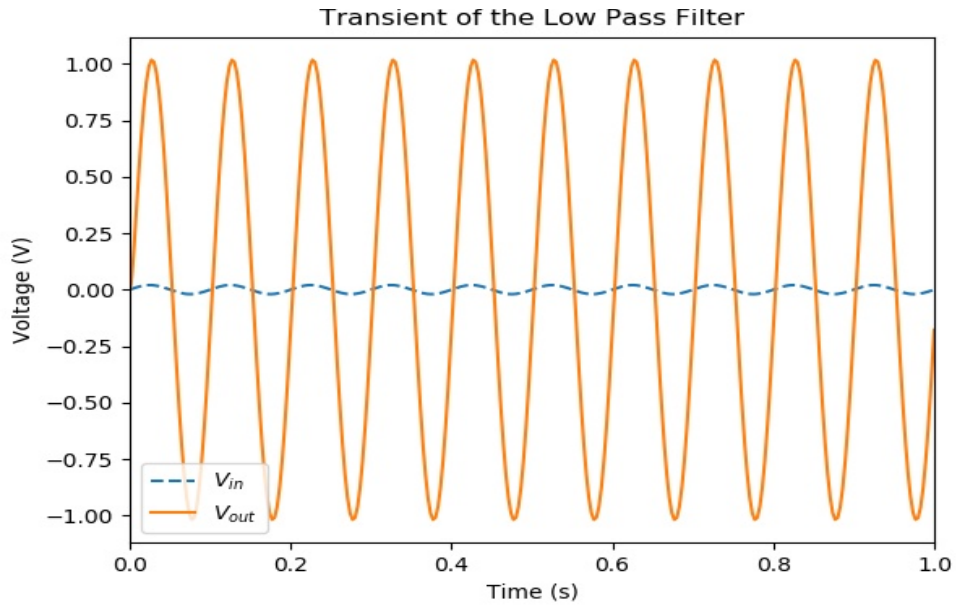
Figure 4.13: Transient response of the circuit shown in Figure 4.12
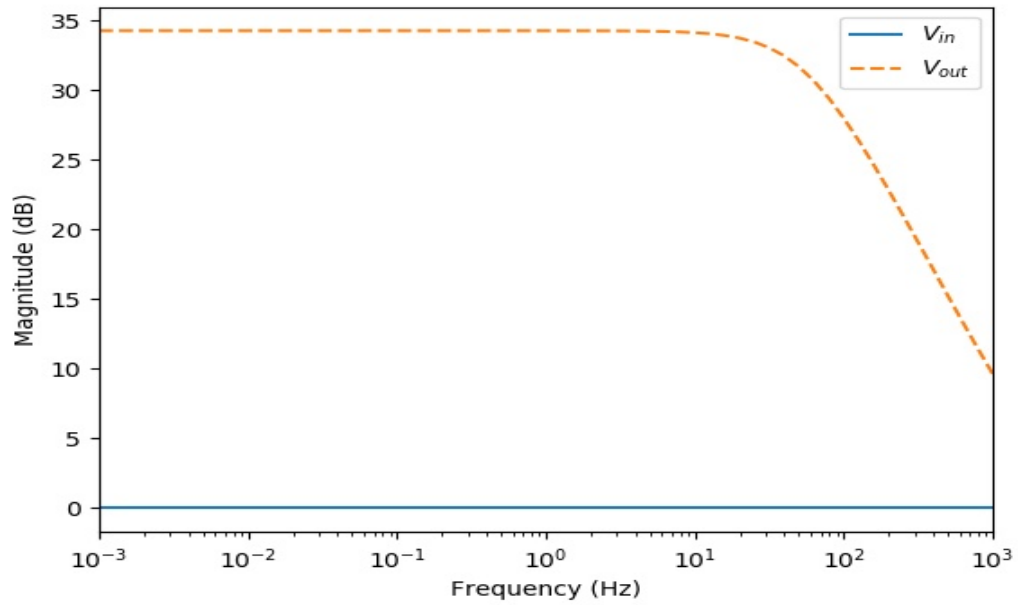
Figure 4.14: Magnitude (in dB) from 1 mHz to 1 kHz for the circuit shown in Figure 4.12
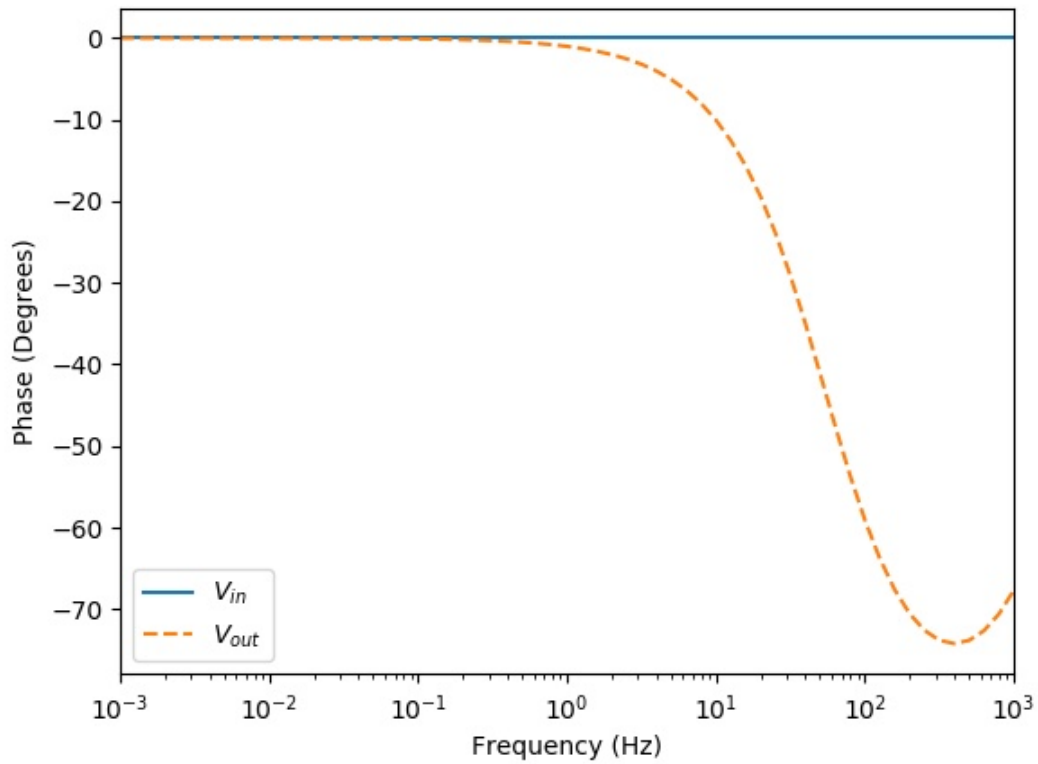
Figure 4.15: Phase (in degrees) from 1 mHz to 1 kHz for the circuit shown in Figure 4.12

4.2.3 Full Circuit

A list of all components used in the amplifier circuit simulation, which is shown in Figure 4.16, can be found in Table 4.1. In this circuit, the output of the high-pass filter is connected directly to the positive terminal of the active low-pass filter. For simplicity, the supply voltages V_S and V_n have been reduced to voltage reference nodes, but are, in reality, provided by an external power supply.

The transient response of the full circuit is shown in Figure 4.17, with traces shown for the original input signal, the output of the instrumentation amplifier, and the final output of the circuit. The results in this graph are reflective of those from the previous tests of the individual stages, with the original signal being amplified to approximately one thousand times its original value. This
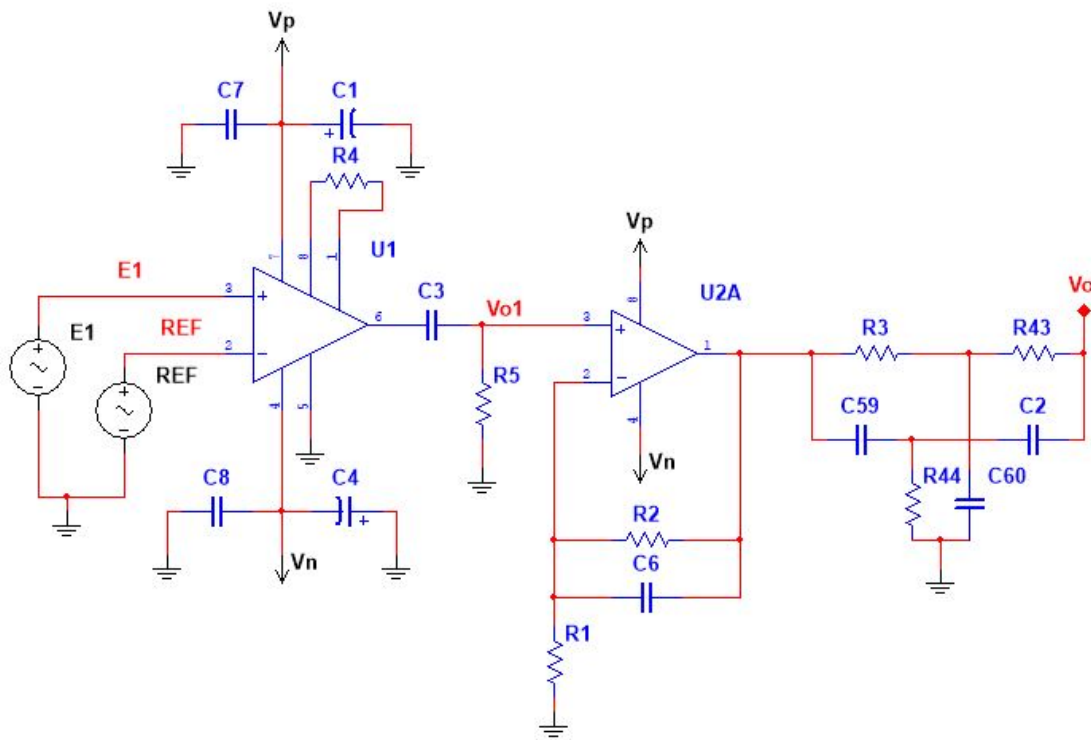
Figure 4.16: Multisim Schematic of the full amplifier circuit.

amplification allows the incoming signal to occupy a greater expanse of the voltage range available through the data collection module, allowing for more precise measurements.
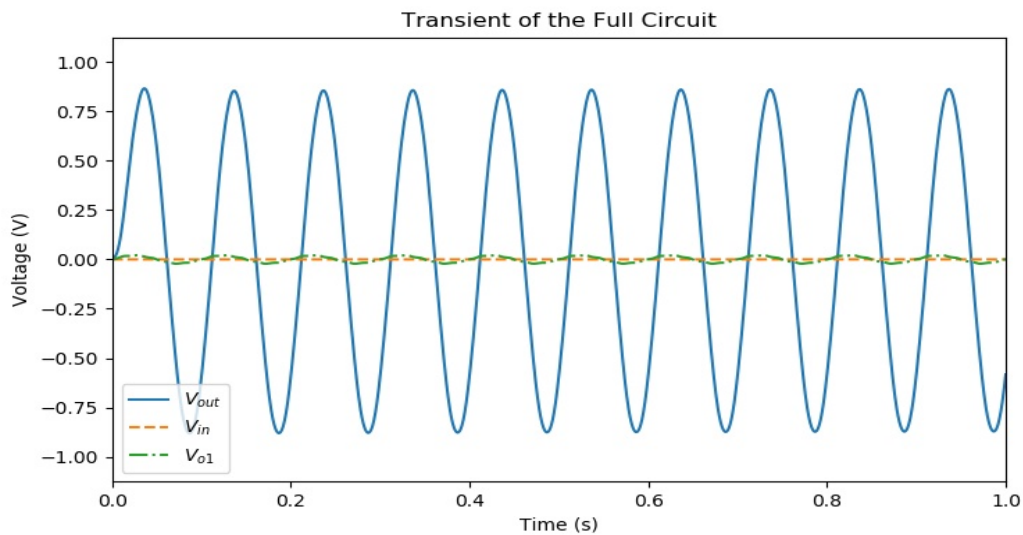
Figure 4.17: Transient response of the full amplifier circuit.

Component	Value	Quantity
Instrumentation Amplifier	Analog Devices AD623BN	1
Operational Amplifier	Texas Instruments TLC277CP	1
C_1, C_4	Tantalum Capacitor, 10 μF	2
C_2, C_{59}	Ceramic Capacitor, 560 nF	2
C_3	Ceramic Capacitor, 10 μF	1
C_6	Ceramic Capacitor, 1 μF	1
C_7, C_8	Ceramic Capacitor, 100 nF	2
C_{60}	Ceramic Capacitor, 1.2 μF	1
R_1	Thick Film Chip Resistor, 62 Ω	1
R_2	Thick Film Chip Resistor, 3.16 kΩ	1
R_3, R_{43}	Thick Film Chip Resistor, 4.7 kΩ	2
R_4	Thick Film Chip Resistor, 499 Ω	1
R_5	Thick Film Chip Resistor, 100 kΩ	1
R_{44}	Thick Film Chip Resistor, 2.32 kΩ	1

Table 4.1: List of components and respective values used for a single amplifier circuit.

Figures 4.18 and 4.19 show the magnitude in dB and the phase in degrees of the original input, of the output of the instrumentation amplifier and high-pass filter, and of the final output of the full amplifier. Because all filtering is performed after at least one stage of amplification, only the smallest of frequencies are reduced to a negligible amount. The frequencies below 0.16 Hz and above 50 Hz are not fully amplified but are not fully removed from the output.
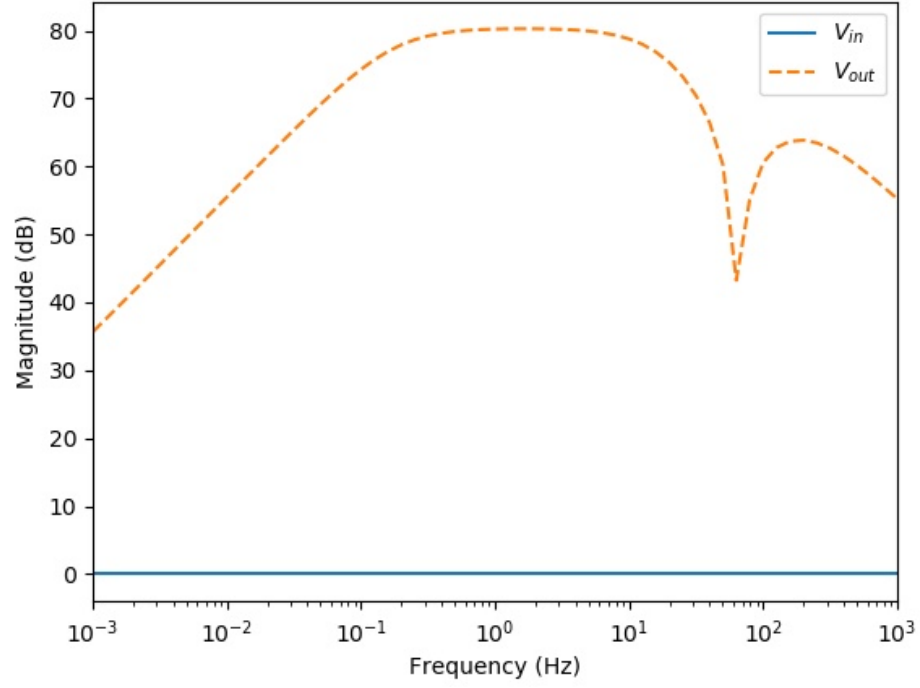
Figure 4.18: Magnitude (in dB) of the full amplifier circuit from 1 mHz to 1 kHz.
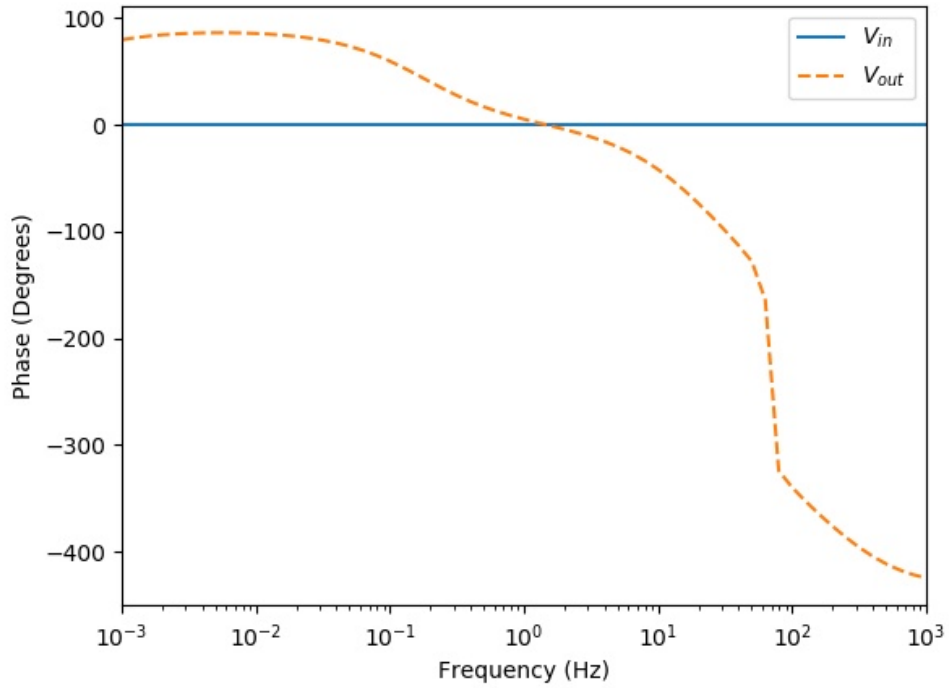
Figure 4.19: Phase (in degrees) of the full amplifier circuit from 1 mHz to 1 kHz.

4.3   Initial Testing

To test this circuit design, the Multisim schematic outlined in the previous section was prototyped on a breadboard and connected to a signal generator and DC power supply. The signal generator used was the Tektronix AFG 3021 single channel arbitrary/function generator, and the power supply was a Hewlett-Packard 6236B triple output power supply. The output of the circuit was displayed using a Tektronix MDO3012 mixed domain oscilloscope. As a note, the mean, minimum, and maximum values shown on the oscilloscope outputs in the following figures are not accurate, as most reflect values obtained from other signal measurements at varying amplitudes. Additionally, for testing purposes, two voltage regulators – specifically the LM7805 and LM7905 from Texas Instruments – were used with the outputs of the DC power supply to step the voltage down from ±12 V to ±5 V.

The amplifier was separated into its two stages for testing. The first stage consisted of the instrumentation amplifier circuitry and the high-pass filter, as shown in Figure 4.20. A ±10 mV sinusoidal signal at a frequency of 10 Hz was used to test this circuit (see Figure 4.21). The magnitude of this signal is far greater than the 10-100 μV signal expected from EEG electrode collection; however, this signal was used due to the limitations of the available signal generator. With a gain resistor value of 499 Ω, which produces a gain of 200 V/V from the AD623 instrumentation amplifier IC, the expected output of this circuitry is a 10 Hz sinusoid with an amplitude of ±2 V, which is reflected in the oscilloscope output shown in Figure 4.22.
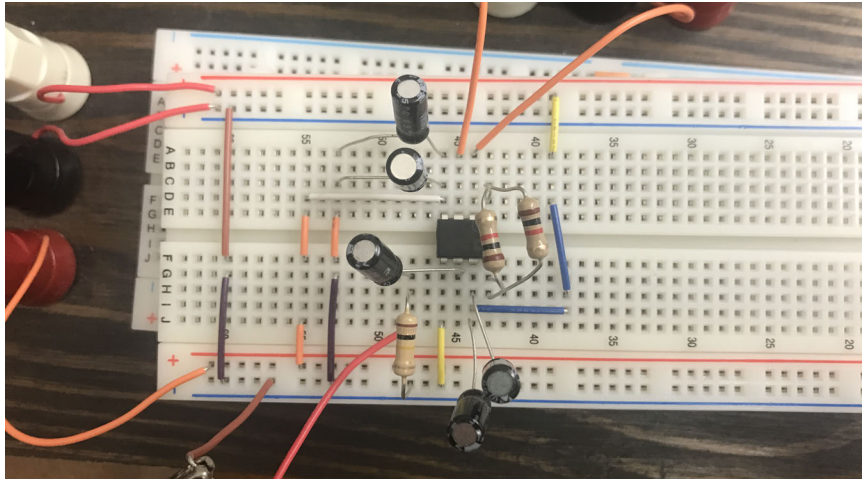
Figure 4.20: Breadboard prototype of the instrumentation amplifier and high-pass filter circuitry.
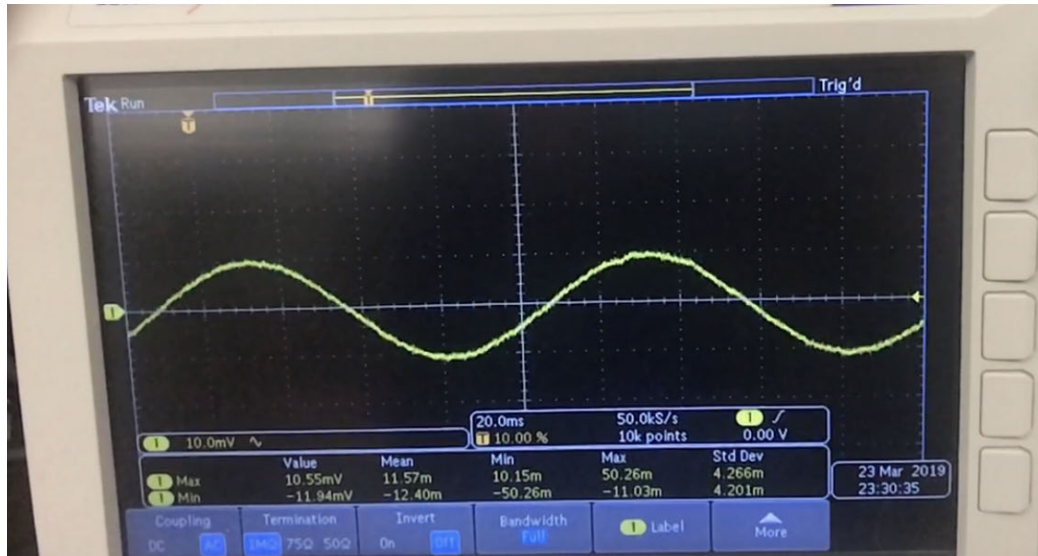
Figure 4.21: The input signal used to test the instrumentation and high-pass filter circuitry – 10 Hz sinusoidal signal with amplitude of ±10 mV.

Figure 4.22: The output signal obtained from the instrumentation amplifier and high-pass filter circuitry – 10 Hz sinusoidal signal with amplitude of ±2 V.

The second stage of the amplifier tested was the low-pass filter circuitry, for which the breadboard prototype is shown in Figure 4.23. Figure 4.24 shows the input signal used to test the second stage, which is a 10 Hz signal with an amplitude of ±20 mV. This signal reflects the expected output of the instrumentation amplifier circuitry when using the true expected signal for the instrumentation amplifier input given by actual EEG data collection. The expected gain of this circuitry is 50 V/V, which should produce an output signal of ±1 V. The oscilloscope output measured at the output of the low-pass filter circuitry shown in Figure 4.25 reflects this expected result.
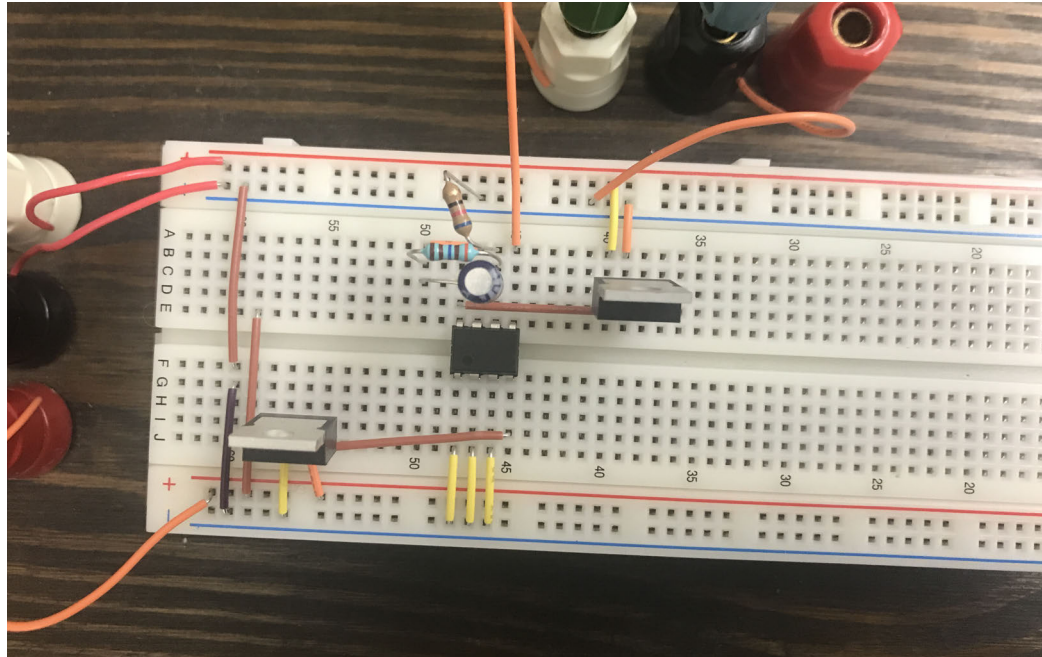
Figure 4.23: Breadboard prototype of the low-pass filter circuitry.
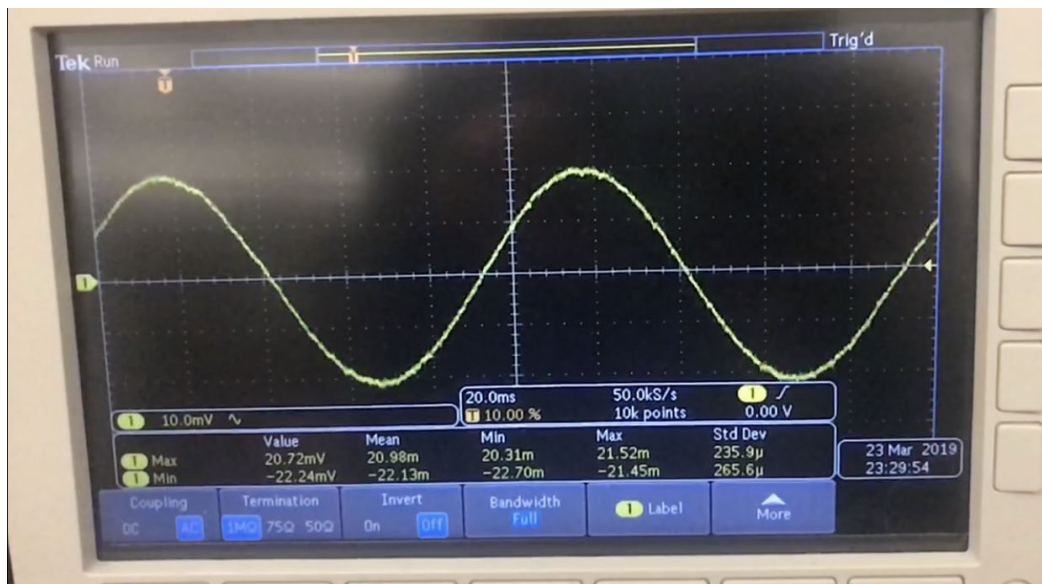
Figure 4.24: Oscilloscope output for direct measurement of the input signal from the signal generator, showing a 20 mV signal at 10 Hz
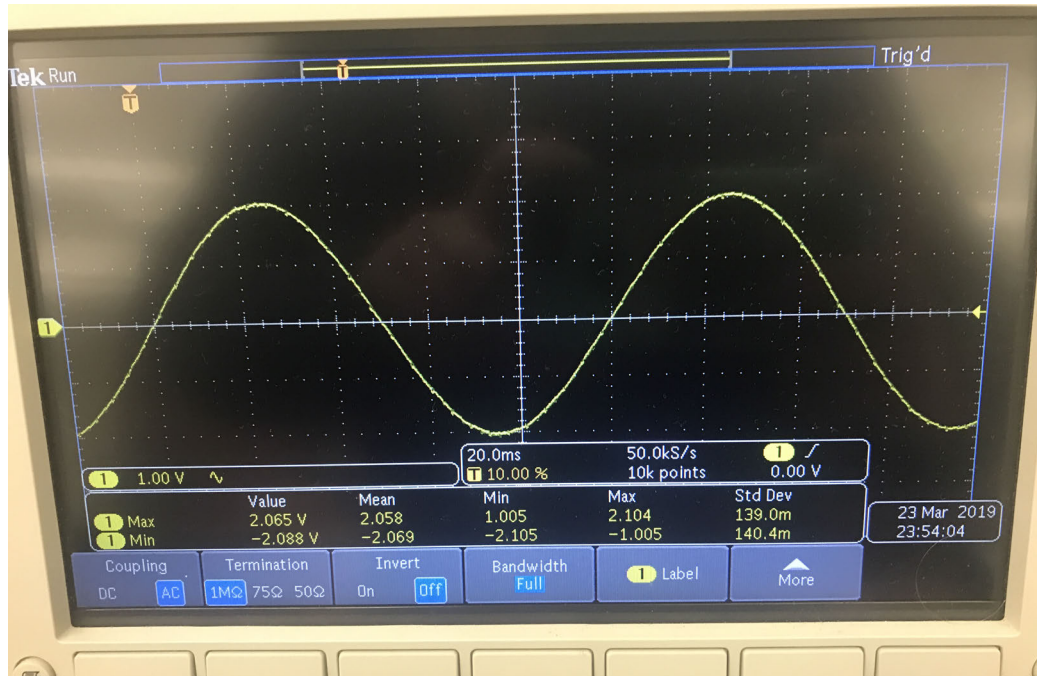
Figure 4.25: Oscilloscope output for the measurement taken at the output of the low-pass filter circuit – 10 Hz sinusoidal signal with an amplitude of ±2 V.

Following successful testing of the two stages individually, the circuits were combined to test the full amplifier. Because of the previously-mentioned limitations of the signal generator, which cannot generate signals smaller than ±10 mV, some modifications were made to the circuit to account for this. Primarily, the gain resistor on the AD623 was changed to a 100 kΩ resistor, which provides a gain value of 2 V/V. This change prevents the output of the amplifier from being clipped once it surpasses the limitations of the selected ICs and of the power supply.

The full breadboard prototype is shown in Figure 4.26. The input signal applied to the full circuit is the same as that shown in Figure 4.21 – a 10 Hz sinusoid with amplitude ±10 mV. The final output of the full circuit is shown in Figure 4.27, which shows a ±1 V sinusoidal signal at a frequency of 10 Hz. These results are promising for future work on this project, which will be discussed in Chapter 5.
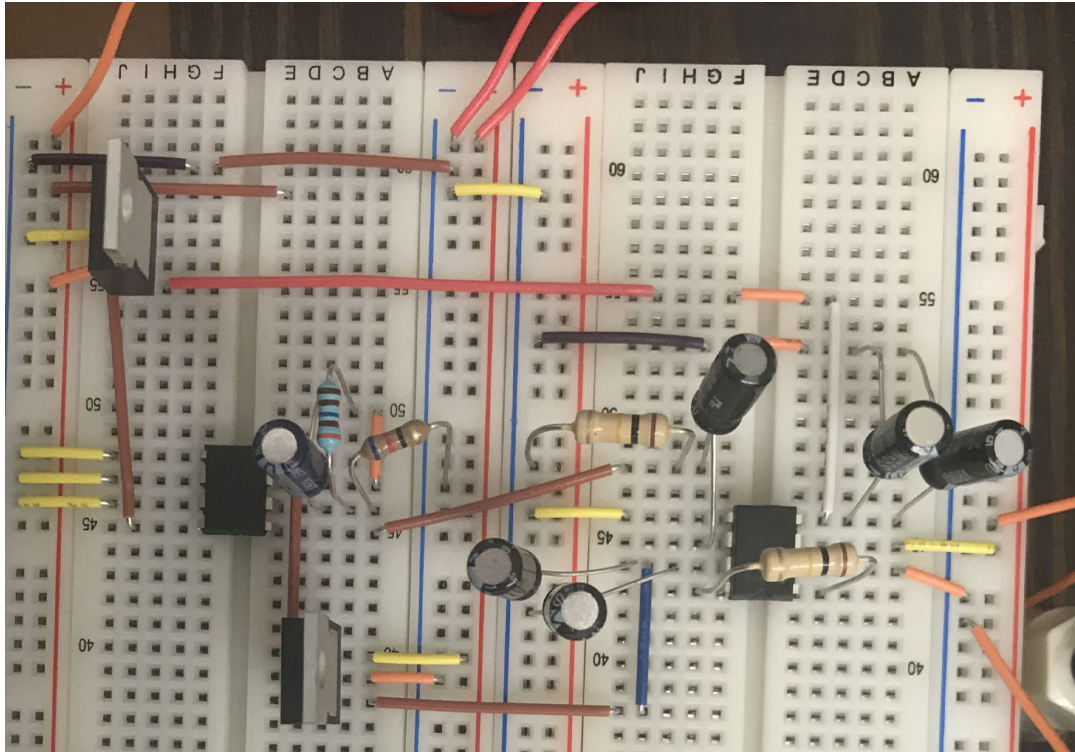
Figure 4.26: Breadboard prototype of the full amplifier circuit.
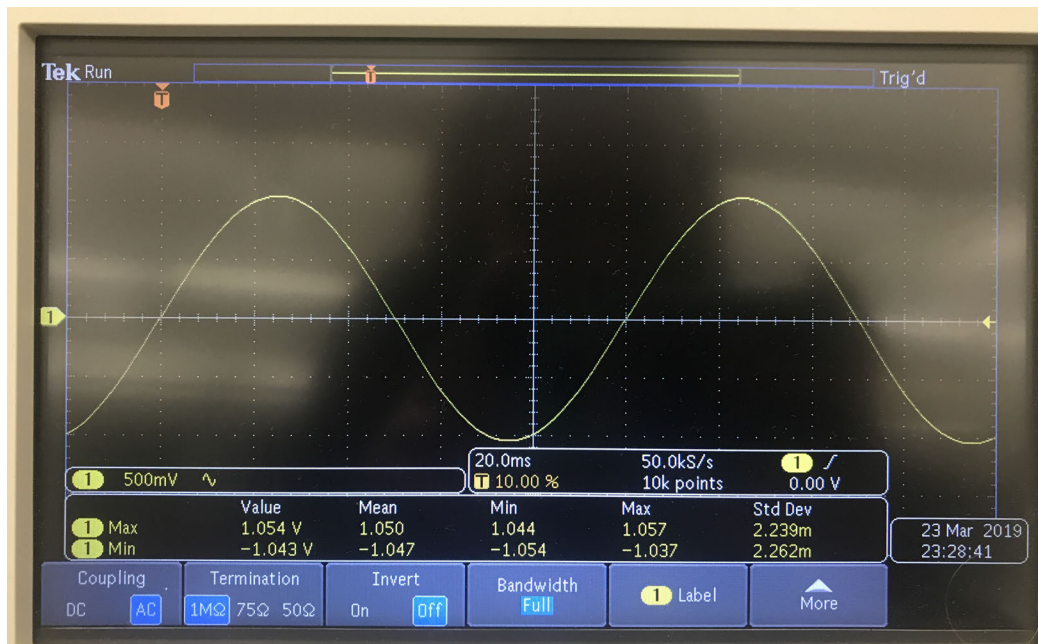
Figure 4.27: Oscilloscope output for the measurement taken at the output of the full circuit – 10 Hz sinusoidal signal with an amplitude of ±1 V.

Chapter 5

Future Work

As mentioned previously, these components are designed to be implemented as part of a larger system. One of the next steps in developing such a system is to create a printed circuit board for the amplifier circuitry. This PCB will contain eight amplifier circuits as outlined in Chapter 4 to provide full access to all eight available input channels on the DAQ. Eight PCB-mount 1.5 mm touch-proof safety sockets will serve as the connectors for the electrodes to the amplifiers. All eight channels will be output through a DB-25 connector, which will be used to connect the circuitry to the collection device. A preliminary version of the PCB design for the amplifier circuits is shown in Figure 5.1. In addition to the amplifier channels, the board will contain circuitry to provide power to the amplifiers via a rechargeable 7.4 V lithium polymer battery, using the design given in [2]. This circuitry is shown in Figure 5.2. The PCB design uses a six-layer board to provide separate power planes for the positive and negative DC power signals and the signal ground, as well as a separate layer to run additional traces for the main circuitry.

Following the completion of the PCB design, printing, and assembly, the group seeks to integrate these systems as part of a larger system for use in EEG-based biofeedback research. This experimental setup will use these systems to provide EEG data to software on the secondary computer
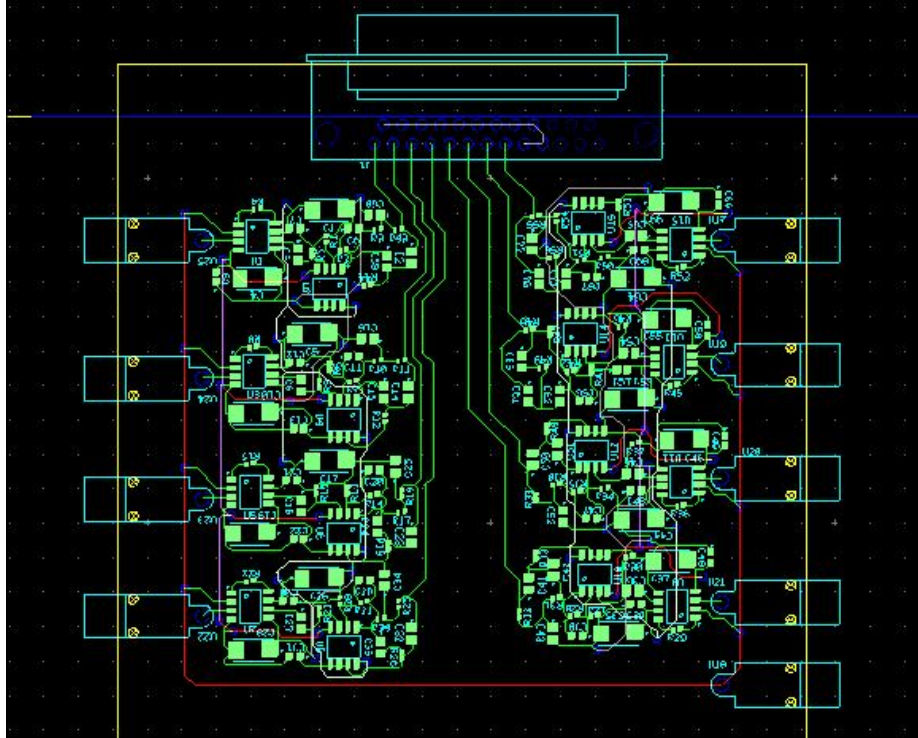
Figure 5.1: Preliminary PCB design of the eight-channel amplifier circuit, showing the 1.5mm touchproof socket inputs and the DB-25 connector output.

described in Chapter 3, which will provide data processing to control a responsive visualization which will be used to study the potential of biofeedback in neuromodulation experiments. Ultimately, the group plans to use the fully-developed system to study the use of visual biofeedback as a therapeutic supplement to pharmaceutical treatments for epilepsy.

Although this research tried to address as many previously-identified or potential challenges in these designs as possible, there is always room for more improvement, especially in terms of selection of the components used in the data collection device. This could range from selecting components with better form factors to even further reduce the size of the device to developing a single stand-alone board which provides only the functions necessary for data collection. Additionally, the amplifier circuitry could be improved by adding adjustable features which allow one to configure the gains and filters of the different stages depending upon the research parameters and targets.
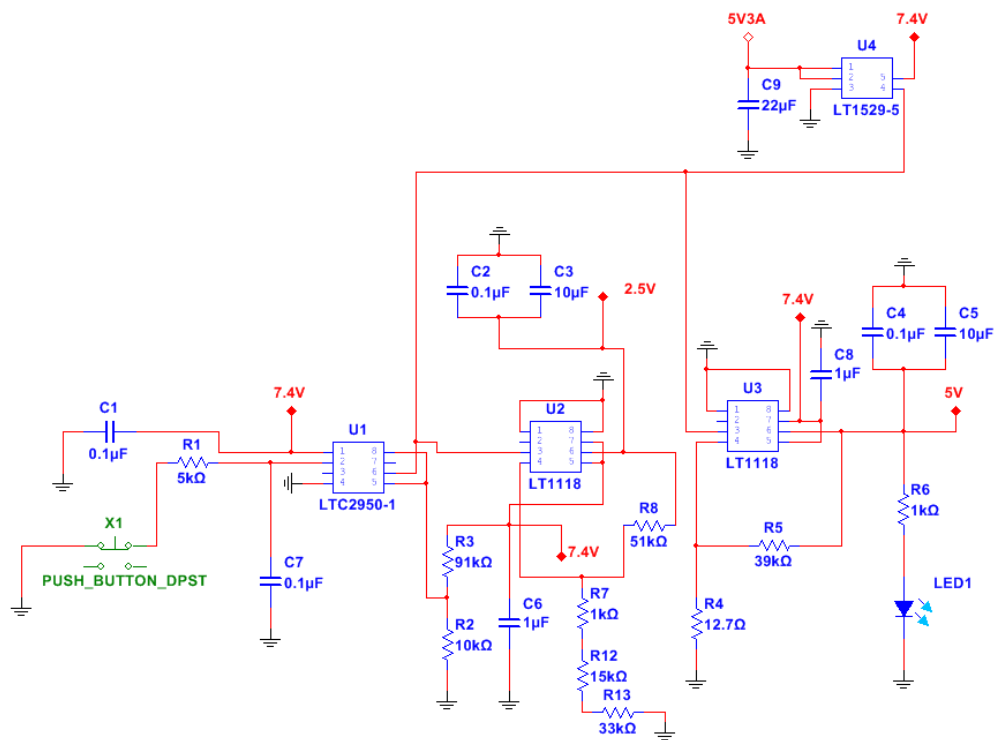
Figure 5.2: Circuit design for the rechargeable lithium polymer battery as given in [2].

Chapter 6

Summary and Conclusions

The designs described in this thesis accomplish the goals defined at the beginning of this research project. The improvements made to the data collection device design address the challenges and limitations outlined in the original research [3]. The new design resolves many of the issues with the previous enclosure, including the instability that resulted in many of the internal components becoming disconnected. The new design also reduces the overall size of the enclosure and standardizes the inputs and outputs. The chosen method of networking between the device and a secondary computer was changed from an ad hoc network to pre-defined WiFi connections, which uses TCP connections to transmit data.

The developed amplifier circuitry is designed to amplify signals with a magnitude of 10-100 μV to the range of ± 1 V, requiring a voltage gain of approximately 1000 V/V. This is accomplished using a two-stage amplifier, the first stage of which is an instrumentation amplifier. The high input impedance and high CMRR offered by the instrumentation amplifier design made it an ideal choice for this application. This implementation provides a voltage gain of 200 V/V. The second stage makes use of an active low-pass filter that provides a gain of 50 V/V to achieve the desired amplification of the signal. In addition to amplification, the circuitry provides some preliminary

filtering at each stage of the amplifier. Specifically, the circuit is designed to attenuate signals below 0.16 Hz and above 50 Hz, with additional filtering of signals close to 60 Hz provided by a notch filter. These filters help to isolate the desired signals from common noise sources that may interfere with data collection.

Although these designs perform well in controlled tests, further testing is required to test the efficacy of their use for the intended purpose of creating a full visual biofeedback system. Specifically, the amplifier circuitry needs to be tested with an input signal that is reflective of typical EEG signals, and the data collection device needs to be tested in a real-time application to ensure that all aspects of the collection and transmission of data function correctly.

Overall, this research covered a broad array of topics, including 3D CAD modeling, computer networking, circuit design, and electronic device design and testing, and provided a better understanding of the engineering design process. In addition to these more practical aspects, this research provided an in-depth understanding of creating documentation for a device that can be used for troubleshooting issues. These preliminary results show promise for future developments in this project, with regard to implementing the full feedback system.

Bibliography

[1] Measurement Computing Corporation, *USB-1608FS-Plus User's Guide*, 2014. Rev. 5A.

[2] Z. Allen, T. Rahmatullah, and T. Ishalaiye, *Innovative Lithium Polymer Battery Powered PCB for Experimentors*. University of Mississippi Department of Electrical Engineering, May 2016.

[3] S. Singh, "Portable Bio-signal Data Logger," Thesis, University of Mississippi, May 2017.

[4] K. Vinecore, M. Aboy, J. McNames, C. Phillips, R. Agbeko, M. Peters, M. Ellenby, M. McManus, and B. Goldstein, "Design and implementation of a portable physiologic data acquisition system," *Pediatr Crit Care Med*, vol. 8, no. 6, 2007.

[5] K. Akingbade, I. Alimi, and T. Oni, "Design of a data logger for biomedical signals," *International Journal of Electronics and Electrical Engineering*, vol. 3, 01 2014.

[6] L. G. Luu, N. P. Nguyen, and T. Vo Van, "Design a customizable low-cost, matlab based wireless data acquisition system for real-time physiological signal processing," in *6th International Conference on the Development of Biomedical Engineering in Vietnam (BME6)* (T. Vo Van, T. A. Nguyen Le, and T. Nguyen Duc, eds.), (Singapore), pp. 313–317, Springer Singapore, 2018.

[7] S. A. Memon, A. Waheed, T. Başaklar, and Y. z. Ider Ider, "Low-cost portable 4-channel wireless eeg data acquisition system for bci applications," in *2018 Medical Technologies National Congress (TIPTEKNO)*, pp. 1–4, Nov 2018.

[8] Trans Cranial Technologies, Wanchai, Hong Kong, *10/20 System Positioning Manual*, 2012.

[9] "EEG (electroencephalogram)." https://www.mayoclinic.org/tests-procedures/eeg/about/pac-20393875. Last Accessed: 2019-03-24.

[10] Anker Innovations Ltd., *Anker PowerCore 10000*.

[11] Raspberry Pi Foundation, *Raspberry Pi Documentation*.

[12] Analog Devices, *AD623*, 2018. Rev. F.

Appendices

Python Code

server_daq.py

```python
from socket import *

from _thread import *

from uldaq import *

from os import system

from sys import stdout

from time import sleep, time_ns

import threading


print_lock = threading.Lock()

def threaded(c):

    try:

        daq_dev = daq_setup()

        low_chan = 0

        high_chan = 7

        range_index = 0

        if daq_dev == -1:

            raise Exception("Error: Could not find DAQ device")

        ai_dev = daq_dev.get_ai_device()

        if ai_dev is None:

            raise Exception("Error: The DAQ device does not support

                analog input")

        desc = daq_dev.get_descriptor()

        print("Connecting to %s - please wait." % desc.dev_string)

        daq_dev.connect()
```

```python
        ai_info = ai_dev.get_info()

        in_mode = AiInputMode.SINGLE_ENDED

        num_chan = ai_info.get_num_chans_by_mode(in_mode)

        if high_chan >= num_chan:

            high_chan = num_chan -1

        ranges = ai_info.get_ranges(in_mode)

        if range_index >= len(ranges):

            range_index = len(ranges) - 1

        system('clear')

        try:

            while True:

                data = c.recv(1024).decode()

                if not data or data == "end":

                    print_lock.release()

                    break

                out = ""

                for channel in range(low_chan, high_chan + 1):

                    out += "%0.6f," % (ai_dev.a_in(channel, in_mode,

                        ranges[range_index], AInFlag.DEFAULT))

                out = "%d,%s\n" % (time_ns(),out)

                c.send(out.encode())

                sleep(0.1)

        except KeyboardInterrupt:

            pass

except Exception as e:

    print("\n%s", e)
```

```python
    finally:
        if daq_dev:
            if daq_dev.is_connected():
                daq_dev.disconnect()
            daq_dev.release()
        c.close()
        interrupt_main()
    return


def daq_setup():
    daq_dev = None
    ai_dev = None
    status = ScanStatus.IDLE
    desc_index = 0
    interface_type = InterfaceType.USB
    try:
        devs = get_daq_device_inventory(interface_type)
        num_devs = len(devs)
        if num_devs == 0:
            raise Exception("Error: No DAQ devices found")
        print('Found %d DAQ Device(s):' % num_devs)
        for i in range(num_devs):
            print("\t%s (%s)" % (devs[i].product_name, devs[i].
                unique_id))
        return DaqDevice(devs[desc_index])
    except Exception as e:
        print("\n%s" % e)
```

```python
        return -1


def Main ():
    HOST = "192.168.2.11"
    PORT = 12000
    s = socket (AF_INET , SOCK_STREAM )
    s.bind ((HOST ,PORT ))
    print ("Socket bound to port %d" % PORT)
    s.listen (1)
    print ("Socket is listening")
    try :
        c, addr = s.accept ()
        print_lock .acquire ()
        msg = c.recv (1024) .decode ()
        if msg == "ready":
            print ("Connected to: %s : %s" % (addr [0] ,addr [1]))
            t1 = threading .Thread (target=threaded ,args =(c,))
            t1.start ()
            t1.join ()
        else :
            print ("Could not establish the connection")
    except (KeyboardInterrupt , ConnectionResetError ) as e:
        print ("Ending program")


if __name__ == "__main__":
    Main ()
```

client_daq.py

```python
from socket import *
def Main():
    HOST = "192.168.2.11"
    PORT = 12000
    s = socket(AF_INET,SOCK_STREAM)
    s.connect((HOST,PORT))
    msg = input("Hit ENTER to begin")
    print("Use CTRL+C to end")
    msg = "ready"
    s.send(msg.encode())
    out_file = open("output_data.txt", "w")
    while True:
        try:
            s.send("c".encode())
            data = s.recv(1024).decode()
            out_file.write(data)
            print(data)
        except (KeyboardInterrupt):
            s.send("end".encode())
            break
    s.close()


if __name__ == "__main__":
    Main()
```